SERDP

INTERIM REPORT III

Extension of the Underwater Munitions Expert System to Beach Face and Estuarine Environments

Sarah E. Rennie
Alan Brandt
Johns Hopkins University Applied Physics Laboratory

August 2021

SERDP Project MR19-1126

REPORT DOCUMENTATION PAGE

Form Approved
OMB No. 0704-0188

1. REPORT DATE *(DD-MM-YYYY)*	2. REPORT TYPE	3. DATES COVERED *(From - To)*
31/08/2021	SERDP Interim Report	4/9/2019 - 4/8/2022

4. TITLE AND SUBTITLE
Extension of the Underwater Munitions Expert System to Beach Face and Estuarine Environments

Interim Report III

5a. CONTRACT NUMBER
19-C-0015

5b. GRANT NUMBER

5c. PROGRAM ELEMENT NUMBER

6. AUTHOR(S)
Sarah E. Rennie
Alan Brandt

5d. PROJECT NUMBER
MR19-1126

5e. TASK NUMBER

5f. WORK UNIT NUMBER

7. PERFORMING ORGANIZATION NAME(S) AND ADDRESS(ES)
Johns Hopkins University Applied Physics Laboratory
11100 Johns Hopkins Road
Laurel, MD 20723

8. PERFORMING ORGANIZATION REPORT NUMBER
FPS-R-21-0xxx

9. SPONSORING/MONITORING AGENCY NAME(S) AND ADDRESS(ES)
Strategic Environmental Research and Development Program
4800 Mark Center Drive, Suite 17D03
Alexandria, VA 22350-3605

10. SPONSOR/MONITOR'S ACRONYM(S)
SERDP

11. SPONSOR/MONITOR'S REPORT NUMBER(S)
MR19-1126

12. DISTRIBUTION/AVAILABILITY STATEMENT
DISTRIBUTION STATEMENT A. Approved for public release: distribution unlimited.

13. SUPPLEMENTARY NOTES

14. ABSTRACT

This status report summarizes recent efforts to build two new versions of the Underwater Munitions Expert System to encompass additional aquatic environments of interest to managers in munitions remediation management: on the beach face and in estuaries. Recent research sponsored by the SERDP Munitions Response (MR) program has completed experiments in the swash zone portion of the sandy coastal region, an energetic environment where munitions are subject to intermittent submergence by waves rushing up the beach face. Other research studies have examined the behavior of munitions located in estuaries where the seafloor sediment often has a large component of cohesive muds. Numerous formerly-used defense sites currently requiring remediation are located in estuarine environments, while the high recreational value of beaches make them a region of particular management concern.

The development of a version of the expert system representing the behavior of munitions under processes in the swash zone is discussed. Due to high variability in observations of burial and migration response, it was difficult to discern physical force balances with clarity; therefore, an aggregate statistical approach was used. In estuaries, the fate of munitions appears dominated by burial, with minimal migration. Physics-based models for impact penetration, and for subsequent burial by settling, are presented, requiring input of geotechnical sediment measurements. Previous research performed under the Office of Naval Research provided guidance for impact burial into the soft seabed, as well as scour burial modeling, which was updated to account for cohesive sediments.

15. SUBJECT TERMS
Underwater Munitions, UXO, UXO mobility, Bayesian Model of Munition Behavior, computer based expert system UnMES, Beach Face, Estuarine Environments

16. SECURITY CLASSIFICATION OF:			17. LIMITATION OF ABSTRACT	18. NUMBER OF PAGES	19a. NAME OF RESPONSIBLE PERSON
a. REPORT	b. ABSTRACT	c. THIS PAGE			Sarah Rennie
UNCLASS	UNCLASS	UNCLASS	UNCLASS	49	19b. TELEPHONE NUMBER *(Include area code)* 443-778-8178

Extension of the Underwater Munitions Expert System to Beach Face and Estuarine Environments

S.E. Rennie, A. Brandt
Johns Hopkins Applied Physics Laboratory

June 2021

Table of Contents

Acronyms and Symbols

BN	– Bayesian Network
B	– burial depth of the UXO
CPT	– Conditional Probability Table(s)
C. I.	- Confidence Interval
D	– Diameter of the UXO
d_{50}	– median sand grain size
f_w	– bed shear friction coefficient under waves
h	– water depth
H_0	– offshore wave height
H_s	– significant wave height
G	– shear modulus of the sediment
k_{bed}	– length of seabed roughness
KC	– Keulegan-Carpenter number, defined in Eq.(2.8)
IMU	– Inertial Measurement Unit
L	– munition length
L_0	– offshore wavelength
LWE	– Littoral Warfare Environment at Aberdeen Proving Grounds, USACE
MBP	– Mine Burial Program
MC	– Monte Carlo
MEC	– Munitions of Concern
MR	– Munitions Response
ONR	– Office of Naval Research
PDT	– probability distribution table
PFFP	– portable free fall penetrometer
QSBC	– quasi-static bearing capacity
R	– maximum runup on the beach face
SERDP	– Strategic Environmental Research and Development Program
S_g	– specific gravity of UXO
s_u	– undrained shear strength
T_p	– wave period
UnMES	– Underwater Munitions Expert System
UXO	– Unexploded Ordnance
v_0	– vertical velocity of UXO at the water-sediment interface
α	– flow angle of attack
β	– angle of beach face
ξ	– Iribarren number, defined in Eq.(2.3)
ϕ_0	– angle of long axis of munition at impact with water-sediment interface
ψ	– contact angle of cylinder with the seabed surface
ρ_{obj}	– density of UXO
Θ_m	– object mobility number, defined in Eq.(2.1)
θ	– Shields number, defined in Eq.(2.8)

Extension of the Underwater Munitions Expert System to Beach Face and Estuarine Environments

Abstract

This status report summarizes recent efforts to build two new versions of the Underwater Munitions Expert System to encompass additional aquatic environments of interest to managers in munitions remediation management: on the beach face and in estuaries. Recent research sponsored by the SERDP Munitions Response (MR) program has completed experiments in the swash zone portion of the sandy coastal region, an energetic environment where munitions are subject to intermittent submergence by waves rushing up the beach face. Other research studies have examined the behavior of munitions located in estuaries where the seafloor sediment often has a large component of cohesive muds. Numerous formerly-used defense sites currently requiring remediation are located in estuarine environments, while the high recreational value of beaches make them a region of particular management concern.

The development of a version of the expert system representing the behavior of munitions under processes in the swash zone is discussed. Due to high variability in observations of burial and migration response, it was difficult to discern physical force balances with clarity; therefore, an aggregate statistical approach was used. In estuaries, the fate of munitions appears dominated by burial, with minimal migration. Physics-based models for impact penetration, and for subsequent burial by settling, are presented, requiring input of geotechnical sediment measurements. Previous research performed under the Office of Naval Research provided guidance for impact burial into the soft seabed, as well as scour burial modeling, which was updated to account for cohesive sediments.

1. Introduction to the Underwater Munitions Expert System

The Munitions Response (MR) program of SERDP is focused on developing innovative methods to characterize, remediate and sustainably administer sites contaminated with unexploded ordnance (UXO) or other munitions of concern (MEC). The possibility of buried UXO presents a significant challenge to site management, as they are difficult to detect. Also of particular concern is the potential for UXO to migrate from their current location into areas with high likelihood of contact with human receptors. The objective of this effort is the construction of a predictive Underwater Munitions Expert System (UnMES) providing computer-based decision support for management of aquatic sites.

UnMES is based upon a Bayesian Network (BN) framework, a useful method of modeling systems with complex relationships in a probabilistic manner, where each relationship is characterized by a conditional probability table (CPT). A common approach to building a Bayesian network is to

train the CPT using a dataset of example cases. Due to the limited amount of field and laboratory datasets applicable to UXO burial and mobility, the alternative approach taken to construct UnMES is utilization of deterministic models developed to capture the first-order physics of the processes of interest. Extensive Monte Carlo (MC) simulations employing these models are run over the relevant combinations of input variable ranges in order to populate the CPTs in UnMES [Rennie *et al.,* 2019].

The Prototype version of UnMES addresses UXO behavior in wave-dominated, sandy coastal environments. Guided by results from multiple SERDP MR projects, the models incorporated in Prototype UnMES encompass knowledge of UXO burial and migration processes in the shoaling and surf zone, for water depths from 2 to 15 m. Munitions at sites of concern have generally been deposited over an extended time period (months to years) and over an area that encompasses different bathymetric and hydrodynamic regimes, from deep water to the beach face. The spatial application of UnMES partitions the site into provinces that have similar sediment and water depth characteristics. This report discusses the application of recent SERDP MR research studies to extend UnMES to include two additional environments: the sandy beach face, and shallow estuaries where the sediments are cohesive.

Storms are the primary drivers of burial and migration events. UnMES, as currently implemented, focuses on the time scale of a single storm event. Burial and re-exposure of bottom sitting objects (UXO, and marine munitions in general) during high-energy wave conditions will be subjected to local burial processes and mobility potential. Over an extended duration, under seasonal weather patterns with repeated storms, far-field morphologic changes to the seabed can occur which can also influence UXO burial [Rennie *et al.,* 2019]. However, consonant with recent experiments in the swash zone and in estuaries, this report will continue to focus on short timescale processes and localized response.

2. Munitions on the Beach Face

Because beaches are popular recreation areas, the presence of munitions in very shallow water or actually on the beach face presents enhanced danger of human contact. In particular, site managers need to know the probability that a munition in shallow water can get washed up onto the beach face. Conversely, will UXO on the beach bury in place, or get transported offshore? The SERDP project MR-2503 at the University of Delaware performed several experiments to study these, and similar questions [Puleo and Cristaudo, 2020]. The first study was at the Aberdeen Littoral Warfare Environment (LWE), a very large outdoor wave flume where hydrodynamic conditions can be controlled. The second experiment was in the field along the shore of Wallops Island, VA where surrogate UXO were deployed over the course of three months.

The region where waves break and surge onto the beach is highly energetic and dynamic, a difficult environment to study. Two subregions can be defined: the breaker zone in water depths around 1 m, and the swash zone, where waves intermittently inundate the beach. Special instrumentation to measure hydrodynamic flow and munitions response in this turbulent environment had to be developed, including Inertial Measurement Units (IMUs) installed in "smart" surrogate munitions to detect motion [Bruder *et al.*, 2018]. During two large-scale laboratory LWE experiments, the swash and breaker zones were heavily instrumented to record details of UXO behavior, along with intensive surveying of munitions locations before and after each run to determine migration, and measure changes in beach morphology. A total of 58 runs were executed, 33 runs during the first experiment (LWE1) in June 2016, and 25 runs in the second (LWE2) later that year. A range of moderate wave forcing was covered with significant wave heights H_s from 0.2 to 1.1 m, and peak wave periods T_p from 3 to 9 s.

Multiple UXO, including a mix of instrumented surrogates and inert munitions, were deployed in each run, with each UXO response recorded as a single case. Eight different types of UXO were tested, covering the relevant range of munitions' sizes and densities, as shown in Table 1.1. The mix of run conditions and test munitions used are detailed in Cristaudo and Puleo [2020], and Puleo and Cristaudo [2020], where bulk summary statistics for maximum swash zone velocities and run up are presented in tables. The summary observations are available for all cases, including the inert munitions. Detailed high-resolution time series of individual UXO movement recorded by the instrumented munitions are still undergoing analysis, and will not be considered in this report.

Table 1.1 Munitions used in Aberdeen LWE experiments and Wallops Island field test
Adapted from Cristaudo and Puleo [2020], Puleo and Cristaudo [2020]

Munition Description	ID	Shape	Density	Diameter	Length	Comments
			ρ_{obj} kg/m^3	(mm)	(m)	
20 mm Projectile	Proj20	cylinder	7990	20	0.750	
40 mm Projectile	Proj40	cylinder	5720	40	0.200	
BLU-26 Cluster	BLU26	sphere	2939	65	0.065	
BLU-61 Cluster	BLU61	sphere	4460	99	0.099	additional densities in field test
81 mm Mortar	M81	cylinder	4180	81	0.481	with & without fins in field test
M151-70 Hydra Rocket	RLT70	cylinder	3320	70	0.405	
155 mm Howitzer	H155	cylinder	4230	155	0.754	
155 mm Howitzer	H155-ld	cylinder	2115	155	0.800	not used in field test

The swash zone observations show very large variability in burial and migration, even for replicate UXO under similar wave forcing. As will be discussed in the following sections, simple force balance parameterizations proved unable to capture most of the observed response. At this stage of understanding, the probabilistic expert system can at best predict the likelihood of general categories of behavior. Figure 2.1 presents a statistical summary of the Aberdeen LWE data. There

were a total 247 cases recorded in the swash zone. Out of that total, 49% remained stationary (moved less than one diameter), and then became at least partially buried in place. Of all cases, 14% migrated onshore, and 37% migrated offshore. Considering onshore or offshore movement separately, the distances traveled were highly variable, with the standard deviation larger than the mean distance,. As expected, the dense munitions were least likely to move; e.g., among observations of the 20 mm projectile (ρ = 7990 kg/m^3), 90% of cases remained stationary. In both onshore and offshore movement, the least dense UXO, (155-mm-ld howitzer with ρ = 2115 kg/m^3) migrated the farthest with maximum observed distances of 5 m onshore, and 20 m offshore.

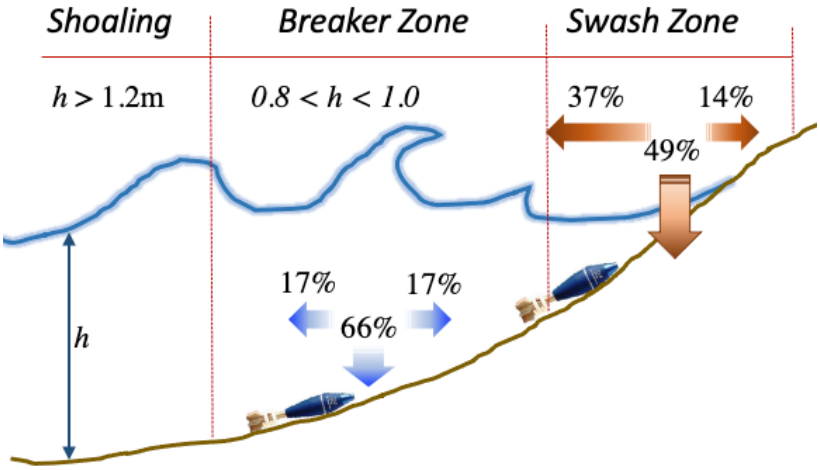

Figure 2.1 Summary of observations from LWE experiments. Down arrow indicates percentage of cases where movement less than 1 UXO diameter was recorded. Arrow to the left (right) shows the percentage observed of offshore (onshore) movement. Note this illustrates an overall summary and does not show the effects of different munition characteristics such as density.

In the less energetic breaker zone, a larger percentage of cases remained stationary. Based on Cristaudo and Puleo [2020], only 34% became mobile, with the direction of movement equally onshore and offshore. The difficulty of tracking UXO movement in the Breaker zone was considerable, and actual migration of munitions may be less frequent (see Section 2.1.2). The migration distances in the breaker zone are also smaller, with a maximum of less than 4 m.

Previous work, e.g. Rennie *et al.* 2017, to understand the physical processes affecting munitions in the surf zone relied on dimensional analysis to infer engineering relationships between environmental forcing and UXO response. A similar approach is pursued here to gain insight into swash zone processes.

2.1 Migration on the Beach Face

The first partitioning is between the UXOs that remain stationary and those that move. Previous work characterized the UXO motion using an Object Mobility number Θ_m [Nielsen, 1993, Rennie

et al., 2017], a parameter formulated in a manner analogous to the Shields number θ, representing the ratio between the mobilizing and stabilizing forces. Θ_m is defined as

$$\Theta_m = \frac{U^2}{gD(\frac{\rho_{OBJ}}{\rho_w}-1)} . \quad \text{Eq. (2.1)}$$

Here the UXO density, ρ_{OBJ}, replaces the sediment grain density used in θ (defined in Eq. 2.8 below), D is the UXO diameter, g is gravitational acceleration, and U represents the relevant near-bed flow velocity. In the swash zone, the flow velocity during uprush and backwash was measured in-situ using an electromagnetic current meter.

2.1.1 Onset of Mobility in the Swash Zone

The critical value of Θ_m, defining the threshold for onset of mobility, has been defined using a power law relationship to the ratio between the UXO diameter D and the stabilizing roughness of the seabed, k_{bed}:

$$\Theta_{m\_crit} = a_1 \left(\frac{D}{k_{bed}}\right)^{b_1} ; \quad a_1 = 1.64 \text{ and } b_1 = -0.71 \quad \text{Eq. (2.2)}$$

The best-fit coefficients $a_1 = 1.64$ and $b_1 = -0.71$ were found in Rennie *et al*. [2017], using an analysis of multiple data sets from underwater studies focusing on motion initiation, and applied in the Prototype UnMES. This critical threshold parameterization is used to predict whether a UXO under a specified forcing is likely to become mobilized. In a non-cohesive sediment, sand grains can be mobilized by the flow, causing scour burial at a bottom-sitting UXO [Friedrichs *et al*., 2016]. If the UXO is partially buried, stronger flow is required to initiate object motion. The influence of partial burial can be incorporated in Eq. (2.2) by setting k_{bed} to the depth of initial burial, B_0, before onset of motion. Similarly, Θ_m can be modified by a burial faction B_0/D as in Puleo and Cristaudo [2020].

During the LWE swash zone experiments, the large majority of UXO were deployed proud at the beginning of the run ($B_0/D = 0$). On occasion (about 10% of the mobility cases), the UXO was left in place partially buried from a previous run ($B_0/D \leq 0.75$). The few mobility cases with complete initial burial were excluded from further analysis.

If UXO behavior in the swash zone is similar to the previous underwater studies, LWE cases categorized as mobile will lie above the critical threshold. An analysis of all LWE cases, with Θ_m computed from bulk statistics of the measured swash uprush velocities, has shown that the previous threshold parameterization does not successfully distinguish mobile conditions from stationary. As shown in Figure 2.1, about half of the UXO cases stayed in place, but only 13% of these stationary cases had Θ_m values that lay below the threshold line defined by Eq. (2.2). Additional nondimensional parameters can be considered to represent additional factors of importance to

movement in the swash zone, such as the Iribarren number, ξ, which incorporates information about both the steepness of the beach face and the wave steepness:

$$\xi = \frac{tan\beta}{\sqrt{\frac{H_0}{L_0}}} \qquad \text{Eq. (2.3)}$$

where β is the angle of the beach face; H_0 and L_0 are the offshore wave height and length respectively. The beach slope was tanβ = 1:16 during LWE1, and slightly steeper at tanβ = 1:10 for LWE2. Another factor of potential relevance represents the areal extent of the UXO presented to the flow, a function of the UXO diameter D and length L, as well as the orientation angle α:

$$\alpha\text{AreaRatio} = \max(|\sin(\alpha)|DL, \pi D^2/4) / DL \qquad \text{Eq. (2.4)}$$

where AreaRatio for cylinders is DL and for spherical objects is $\pi D^2/4$.

It should be noted that most of the data used to form the empirical mobility threshold [Rennie *et al*., 2017], were either from cylinders positioned with their long axis perpendicular to the flow (α = 90º), or on spheres (no preferred orientation). In contrast, during the LWE swash zone experiment about a quarter of the UXO were deployed at a smaller angle to uprush velocity, many of them parallel to the flow (α = 0º). The area presented by the UXO is important in the swash zone, where the area of impact for the surge force can play a larger role than for fully submerged munitions, where the drag force is dominant [Puleo and Cristaudo, 2020] .

Using a combination of the parameters Θ_m, ξ, and αAreaRatio, an onset of motion threshold for the Aberdeen LWE data is found in a power law form that improved the ability to predict mobile conditions in the swash zone:

$$\Theta_m \xi \alpha\text{AreaRatio} = a_2 \left(\frac{D}{k_{bed}}\right)^{b_2} \quad ; \quad a_2 = 6.1 \text{ and } b_1 = -0.83 \qquad \text{Eq. (2.5)}$$

This threshold line, plotted in Figure 2.2, correctly categorizes 72% of the swash cases as either mobile or stationary. In Figure 2.2, the stationary cases are plotted mostly below the threshold, while the majority of the cases where migration > 1D lie above the critical line.

Table 2.1 shows the error matrix [Fawcett, 2006] for classifying mobility using the non-dimensional parameters in Eq. (2.5). By combining information about the hydrodynamics, the UXO properties, and the geomorphic setting, UXO movement was correctly predicted 76% of the time (the True Positive Rate (TPR), or sensitivity). The True Negative Rate (TNR), or specificity, is 67%, for an overall accuracy of 72%. This is an improvement over a situation of no knowledge, which, in this binary classification, would be the 50% of a uniform distribution, however, there is significant unexplained behavior remaining.

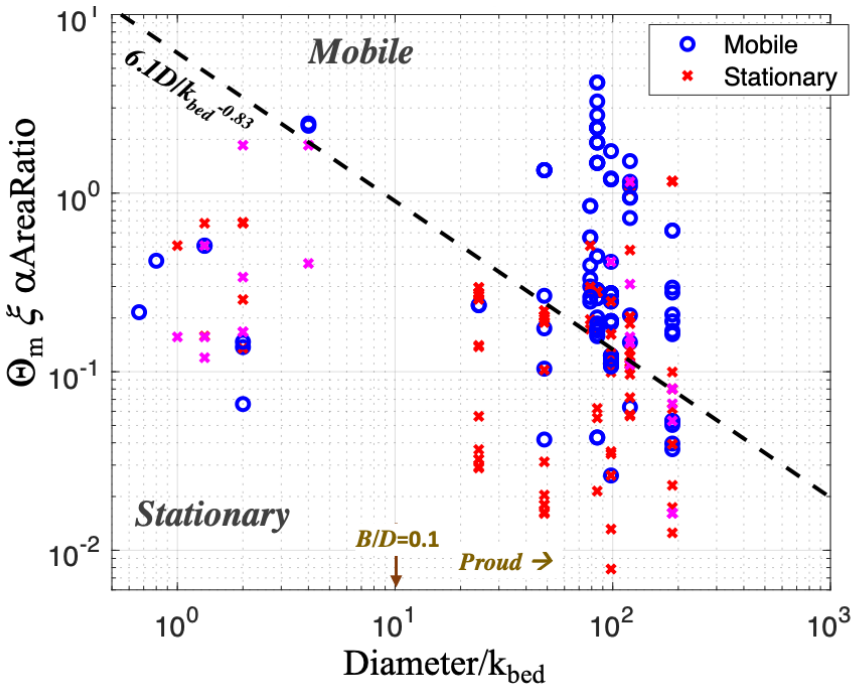

Figure 2.2 Parameter for onset of motion in the swash zone for LWE observations of motion (circle) and no motion (x). Magenta x indicates movement less than 1*D*, treated as stationary. Black dashed line indicates empirically determined threshold.

Table 2.1 Error Matrix for Classification of Mobility in Swash Zone

n=233	Predicted: Stationary	Predicted: Mobile		Accuracy = 0.72
Actual: Stationary	TN = 80	FP = 38	118	Specificity (TNR) = 0.67
Actual: Mobile	FN = 28	TP = 87	115	Sensitivity (TPR) = 0.76
	108	125		

Determining conditions when UXO may become mobilized is an important branching in the code to construct UnMES. However, scour burial can be occurring prior to the wave forcing increases to the critical point of mobilization. During that time, the relevant value of k_{bed} could be increasing. This time-dependent aspect of burial versus mobility, depending on both the time scale of burial and the rapidity of storm onset [Traykovski and Austin, 2017], is addressed in the Prototype version of UnMES by a node representing the rate of wave increase [Rennie *et al.*, 2019]. The onset of motion threshold is extremely sensitive to the specification of k_{bed}. In plotting Figure 2.2, all proud munitions placed on the seabed just prior to the run were assigned for k_{bed} the bed roughness length $2.5*d_{50}$ [Soulsby, 1997], where d_{50} indicates the median sand grain size (0.33

mm for LWE). Points from these proud munitions lie to the right of $D/k_{bed} = 20$. For partially buried UXO, k_{bed} is set to the depth of burial prior to the run. Even a small degree of burial would shift the points significantly to the left. The smallest burial amount resolved by the LWE measurements was $B/D = 0.1$, or $D/k_{bed} = 10$. For the larger diameter UXO considered, at $B/D = 0.1$ the mobility threshold is an order of magnitude larger than when the UXO is proud ($B/D = 0$). Clearly, the ability to accurately predict UXO burial is crucial to be able to estimate onset of motion by means of Eq. (2.5).

In addition, the complexity of the 3-factor critical threshold predictor (Eq. 2.5) renders it less useful in an operational setting. The required parameters are very sensitive to the component values, many of which would not be accurately known in the real-world application for which UnMES is designed. In particular, while the velocity of swash zone flow U was measured in-situ during LWE, in UnMES U would need to be estimated from more generally available observations. As the uncertainty for each factor compounds, the resulting prediction could, in some situations be no better than that from an uninformed uniform distribution. The challenge of obtaining relevant foreshore data for use in the expert system, along with the state of CFD modeling of swash zone hydrodynamics is discussed in Section 2.3.1.

2.1.2 Onset of Mobility in the Breaker Zone

UXO behavior in the breaker zone, where the munitions are continuously submerged, is likely to be more similar to previously-studied shoaling and surf zone regions than to burial and mobility processes in the swash zone. Based on statistics from all cases, under the same wave forcing when half the swash zone munitions migrated, Cristaudo and Puleo [2020] reported about a third were mobilized in the breaker zone (Figure 2.1). To correctly assess breaker zone mobility however, it is essential to understand that locating and surveying munitions in one meter water depth proved to be difficult. Very little GPS survey data were successfully collected during LWE1. A subset of breaker zone munitions was instrumented with IMU. In the LWE2 cases, motion was determined both by use of internal IMU in the instrumented munitions, and by GPS surveys. The correlation between these two mobility measurements is not strong, with $r^2 \leq 0.30$, illustrating the uncertainty inherent in these mapping techniques. A similar analysis of the swash zone IMU versus survey measurements showed an improved correlation ($r^2 = 0.62$ for cross-shore movement).

Another important distinction is between onset of motion that leads to migration, and the small motions that may occur during burial. It was observed during scour burial experiments that the munitions may roll into the developing scour pit as part of the burial process [Rennie *et al*. 2017]. In order to separate the LWE cases into stationary and migrating categories, a threshold distance of one diameter is imposed. (This differs from the criterion used in Puleo and Cristaudo [2020], where any movement larger than 0.05 m is categorized is mobile).

A mix of 81 mm mortars, M151-70 Hydra rockets, and a few 155 mm Howitzer instrumented surrogates were deployed in the breaker zone. Of this group, numbering over 250 cases, movement > 1*D,* as determined from the IMU, was recorded in only 27 cases, or about 10%. A slight majority of these mobility cases moved offshore, although the largest migration distance (1.8 m) was in the onshore direction. Complicating comparison of these data with the proposed mobility threshold is the fact that generally the breaker zone munitions were left in place in between runs, rather than repositioning them proud on the seabed. Therefore, the initial burial depth for most samples is poorly known but assumed to be $B_0 > 0$. As discussed in the previous section, prediction of mobility is very sensitive to burial, so that without burial measurements, breaker zone mobility potential can only be roughly bounded. Survey data from LWE2 indicates highly variable depth measurements, trending downward a few centimeters per run.

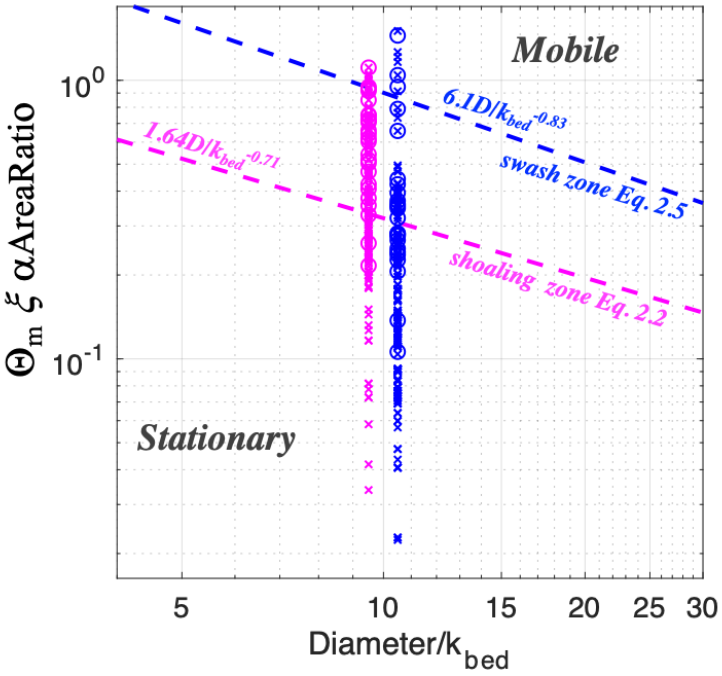

Figure 2.3 Non-dimensional parameter $\Theta_m \xi \alpha$AreaRatio for onset of motion in breaker zone. Blue line indicates threshold for swash zone; magenta threshold from previous shoaling zone analysis.

In Figure 2.3, possible parameterized thresholds for mobility are tested using a consistent assumption of 10% initial burial, $B_0/D = 0.1$. The blue threshold line is that found in the previous section for the swash zone (Eq. 2.5), corresponding to the blue markers representing the combined parameter $\Theta_m \xi \alpha$AreaRatio applied to the breaker zone data, for which U represents the maximum near bed flow velocity, and the orientation angle $\alpha = 90°$. Alternatively, the critical mobility parameterization (Eq. 2.2) used in the Prototype version of UnMES, appropriate for the shoaling region [Rennie *et al.* 2017, 2019], is applied to the breaker zone data, and plotted in magenta. For

both calculations, the circles represent mobile cases, while the x's indicate that no motion was observed. Neither criterion does a satisfactory job of separating mobile from stationary cases. The swash zone threshold in Eq. (2.5) is too high, classifying only 12% of the mobile cases correctly; the lower shoaling region threshold correctly predicts 97% of the mobile cases, but most of the stationary cases are calculated to be in the mobile category. The correct mobility threshold for the breaker zone likely lies in between these two, representing a behavior intermediate to the shoaling and swash zones. At present there is no viable model to appropriately represent the onset of mobility in the breaker zone.

2.1.3 Migration Distance

In the Aberdeen LWE swash zone data, about half the cases became mobilized with 125 observations where migration distance was greater than the UXO diameter. Of these cases, the majority moved offshore (positive direction), with downslope movement noticeably dominant during LWE2 when the beach slope was steeper (tanβ = 1:10). The likelihood of mobility, and the direction of migration for all LWE observations are summarized in Table 2.2.

Table 2.2 Statistics for Onset of Mobility, Direction and Migration Distance in Swash Zone

	Overall		Average Distance	LWE1 tanβ=1:16		Average Distance	LWE2 tanβ=1:10		Average Distance
total = 247	count	%overall	(meters)	count	% in LWE1		count	% in LWE2	(meters)
Stationary	122	49%		65	58%		57	43%	
Mobile	125	51%		48	42%		77	57%	
Onshore	35	28%	-1.1	21	44%	-1.0	14	18%	-1.2
Offshore	90	72%	3.2	27	56%	4.6	63	82%	2.6

Overall, motion was slightly more likely during LWE2. As expected, given the beach slope, offshore-directed migration distances were farther on average than those directed onshore. The largest cross-shore distances, *DistX*, were recorded for the least dense UXO, the 155 mm howitzer "H155-ld" with ρ_{OBJ} = 2115 kg/m^3, for whom offshore migration *DistX* > 15 m was observed in several cases. Note that this very light UXO was deployed only during LWE1, so that its movement on the steeper beach face during LWE2 was not observed. H155-ld was also not included in the Wallops Island field test.

As discussed in Section 2.1.1, previous analysis of underwater munitions behavior had reasonable success in predicting onset of motion. Total migration distance, however, has continued to be difficult to accurately predict. The development of a satisfactory model for UXO migration has been hampered by a lack of field observations of migration coincident with measurements of hydrodynamic forcing. At most coastal sites, experiments have observed burial in place occurring much more frequently than migration [Rennie *et al.,* 2019]. The most extensive migration field set

was obtained in the surf zone at Long Point, Martha's Vineyard, during 2014 [Traykovski and Austin, 2017], where substantial migration distances of over 100 m were observed, with mean cross-shore movement close to 60 m. The existing process model for migration distance in UnMES assumes than the speed of UXO migration, after onset of motion, varies as $(U - U_{crit})^3$, where U_{crit} is found from the critical threshold as in Section 2.1.2. The scaling coefficients and event duration were empirically tuned to match the 2014 Long Point migration observations. It has been determined that a brute force approach, predicting migration distance by integrating estimated UXO acceleration, is likely to be overwhelmed by error accumulation.

Attempts at validation of the preliminary surf zone migration model have not been successful. A single example of significant migration distance observed during the WIMMX experiment [Calantoni, 2018] did not accord with the predictions of the model, perhaps due to presence of consolidated cohesive sediments with reduced bottom roughness. A second field test was conducted in the Long Point surf zone in the fall of 2018 deploying similar surrogate UXO to those of the 2014 test. However, in spite of stronger waves, very little migration was recorded. An analysis by Traykovski and Jaffre [2020] shows a clearly different set of processes was dominant during the 2018 test. Traykovski proposes a complex balance between onshore forcing by wave asymmetry and skewness, and offshore forcing by return flows, to explain the observations. A new SERDP project, MR21-1341 [Traykovski and Palmsten, 2020], will investigate whether wave-averaged models with parameterized versions of the high order wave statistics are adequate to represent the migration behavior. If so, it may be possible to populate UnMES CPTs for the migration nodes in the surf zone using wave-averaged model exploration.

For the swash zone, Cristaudo and Puleo [2020] examined whether some combination of the non-dimensional parameters considered for onset of motion could explain the highly variable observations of migration distance, *DistX*. The object mobility number Θ_m, incorporating the hydraulic forcing and the UXO size and weight, was somewhat effective in categorizing onset of motion in the swash zone (Section 2.1.1); however, minimal relationship was found between Θ_m and *DistX* (Figure 2.4a). Correlation with Θ_m using several formulas, including a modification to account for initial burial, were no higher than $r^2 = 0.08$. As with the 2018 Long Point surf zone results, LWE observations do not support the simple intuitive concept that larger migration distances correspond to stronger wave forcing.

The statistics in Table 2.2 suggest that steeper beach slope encouraged offshore motion; however, measured distances are generally smaller during LWE2. Fits involving $\tan\beta$ parameters have very low correlation with distance. One might expect $\tan\beta$ influence to operate differently for onshore and offshore-directed movement; in fact, the dominant processes during the uprush and backwash phases of the swash event may be quite different. However, even when separated into on- and off-shore cases, correlation within the LWE data set between *DistX* and ξ is found to be minimal.

Another factor that might be important is the duration of the run, assuming that migration can continue further during extended runs. LWE runs were conducted over times ranging from 2.5 to 10 minutes. An examination of *DistX* versus duration shows minimal correlation, with the general trend opposite of expected (shorter distance during longer runs). A closer examination of motion patterns using the detailed IMU time series showed that migration proceeded by oscillating on and offshore for the first several waves; however usually after 120 seconds, the UXO became stuck at its final fixed position, even if the wave forcing continued.

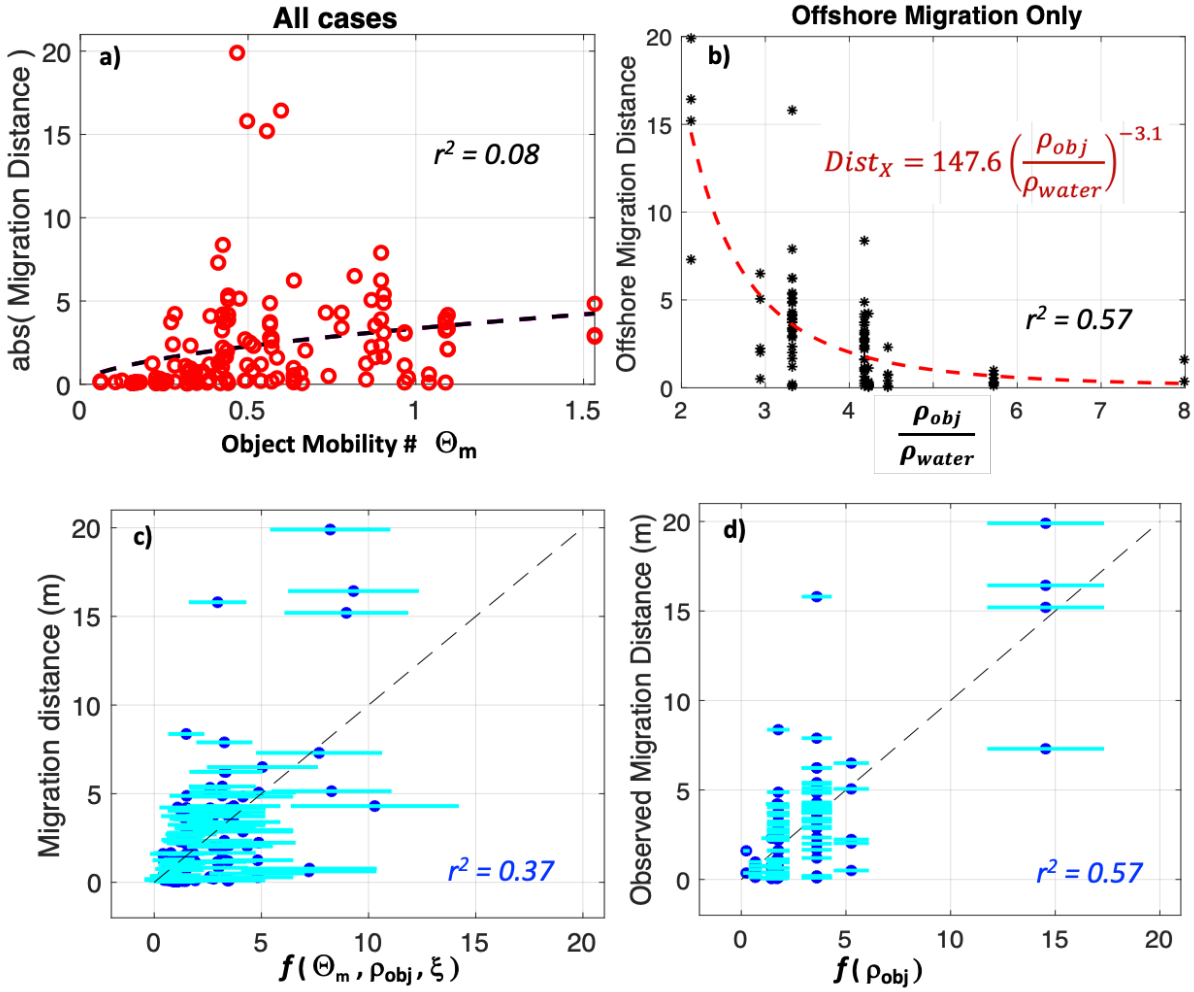

Figure 2.4 Parametric fits to swash zone migration distance: a) all observations versus Θ_m, b) offshore migration only versus UXO density, c) multi-parameter fit for all observations with 95% confidence interval shown in cyan, d) UXO density fit with 95% C.I. for offshore migration.

By far, the single most influential factor in explaining migration distance within the LWE data set is UXO density, with overall $r^2 = 0.23$. When separated into on- and off-shore migration, the correlation of distance with density increases; in fact, for the offshore cases, $r^2 = 0.57$ as shown in Figure 2.4b (onshore cases alone have $r^2 = 0.24$). In Cristaudo and Puleo [2020], an overall best fit was found for a combination of Θ_m (modified by initial burial), ρ_{OBJ} , and ξ, of the form

$$|Dist_X| = a_3\,\Theta_{m\_mod}{}^{b_3}\left(\frac{\rho_{obj}}{\rho_{water}}\right)^{c_3}\xi^{d_3} \qquad \text{Eq .(2.6)}$$

yielding only modest correlation ($r^2 = 0.37$) with the empirical regression coefficients { a_3 =60.8, b_3,=0.5, c_3,=-2.3, and d_3=-0.14 }. This complicated parameterization is unsatisfactory for a number of reasons. The ξ exponent (d_3) is estimated to be negative, indicating an inverse relationship between beach slope and distance, counterintuitive to our physical understanding. Also, given the limited degrees of freedom (sample size = 125), there is sizable uncertainty for each coefficient. Figure 2.4c plots the predictions from Eq. (2.6) with the 95% confidence intervals. It can be seen that the 3-parameter function does an especially poor job of predicting the larger migration distances.

If the regression is restricted to consideration of offshore migration only, the migration behavior is reasonably well captured using a simple relationship to UXO density from Figure 2.4b is:

$$Dist_{Xoffshore} = a_4\left(\frac{\rho_{obj}}{\rho_{water}}\right)^{b_4} \qquad \text{Eq. (2.7)}$$

replotted in Figure 2.4d with the uncertainty range in the coefficients shown as cyan bars. This formula with {a_4=147.6, b_4= -3.1} explains just over half of the observed offshore migration distance variability. Unfortunately, no good predictor for direction of movement has been developed, so that the separation into onshore and offshore migration from run conditions and UXO characteristics remains unknown.

Of the large variability in migration observations in the swash zone, both in distance and directions, only a modest portion can be accounted for by a simple parametric approach representing the bulk hydrodynamics, large scale beach morphology, and munitions characteristics. For the preliminary implementation of a swash zone version of UnMES, it is proposed to retain the uncertainty from these fits by varying each coefficient within the Gaussian distribution defined by its 95% confidence interval when applying these parametric relationships to build the CPTs that define the conditional relationships in the Bayesian Network (see Section 2.3.2).

2.2 Burial in the Swash and Breaker Zones

The potential for munitions to bury in the beach is of particular concern to site management because buried UXO are not easy detected. Also, in order to predict migration, an accurate estimate of burial is required. Most studies have focused on determining the equilibrium depth of burial that an object would reach under prolonged, steady conditions [Friedrichs *et al.*, 2016]. In non-cohesive sediments, scour burial commences as soon as any significant flows begin around a bottom-sitting object. Even a small amount of burial strongly suppresses object mobility; therefore, in order to predict the onset of motion, one needs to understand the rate of burial, in addition to the ultimate burial depth.

The scour burial model currently implemented in UnMES is based on equilibrium burial observations summarized in Friedrichs *et al.* [2016], a data set encompassing conditions under moderate shoaling waves and alongshore currents. Two dimensionless parameters, the Shields number θ, and the Keulegan-Carpenter number KC, defined as

$$\theta = \frac{\frac{1}{2} f_w U^2}{g(\frac{\rho_{sed}}{\rho_w} - 1) d_{50}} \qquad \text{and} \qquad KC = \frac{U T_P}{D} \qquad \text{Eq.(2.8)}$$

were shown to have a significant relationship ($r^2 = 0.85$) with equilibrium burial of the form

$$B/D = a_5 \theta^{b_5} c_5 KC^{d_5} f(\alpha) \qquad \text{Eq.(2.9)}$$

The scour model implementation in Prototype UnMES uses the coefficients {a_5=1.8, b_5=0.33, c_5= 0.10, and d_5= 0.51} for this empirical predictive model. The friction factor under waves, f_w, is computed as in Demir and García [2007], and generally has a value $f_w < 0.01$. Inclusion of a KC factor represents the oscillatory effects, with the upper range of KC bounded at a value of ~100, above which the flow is considered essentially steady. The additional factor accounting for the orientation of munitions to the flow is implemented as

$$f(\alpha) = e^{-2.5(\cos\alpha) - 0.6} \quad \text{for } \alpha < 58°; \quad f(\alpha) = 1 \quad \text{for } \alpha > 58° \qquad \text{Eq. (2.10)}$$

based on laboratory studies from Cataño-Lopera and García [2007], where α is the angle between the UXO long axis and the flow.

The range of θ explored in Friedrichs *et al.* [2016] was for low to moderate energy regimes of clear-water and live-bed scour, and does not cover high-energy conditions where the bed fluidizes the sheet flow regime, usually considered to occur for $\theta > 0.8$. In contrast, Shields numbers reported for the swash zone ranged from $1 < \theta < 8$, indicating a very different, significantly more energetic, regime. Note that the friction factor used for the swash zone is larger, fixed at $f_w = 0.03$ [Puleo and Holland, 2001]. A recent evaluation of friction coefficients in the inner surf and swash zones revealed a wide range (0.005 to 0.04) [Puleo *et al*., 2020] which will lead to significant uncertainty in θ. In these energetic conditions, the dominant physical processes causing burial are expected to be different, including sheet flow forcing and the potential for bed fluidization. Burial by scour alone, driven by the disturbing presence of the object on the seabed, does not continue after the object is fully buried. About 10% of the observations in the LWE data set showed deeper than full burial, indicating that other burial processes are playing a role. A common measurement of swash energy, maximum runup (R), which is often a valuable quantifier of wave-driven impact on a beach, was recorded during the LWE runs. However, no significant relationship was found between burial observations and the magnitude of R.

Comparison of the Aberdeen LWE burial observations to the semi-empirical relationships of Eq. 2.9 found little correlation with the Shields parameter and a moderate correlation with KC [Cristaudo and Puleo, 2020]. This agrees with the conclusion in Friedrichs *et al.*, [2016], that the

main factor under waves alone was KC, representing the relative size of the oscillatory vortices acting on the munitions. A re-analysis of the swash zone burial data, limited to observations with zero initial burial, finds the best fit to be very similar to the KC factor in Eq. (2.9): $0.07KC^{0.50}$ with $r^2 = 0.42$, plotted in Figure 2.5a. This square root relationship with KC was also found in studies of pipeline burial under waves by Sumer and Fredsoe [1990].

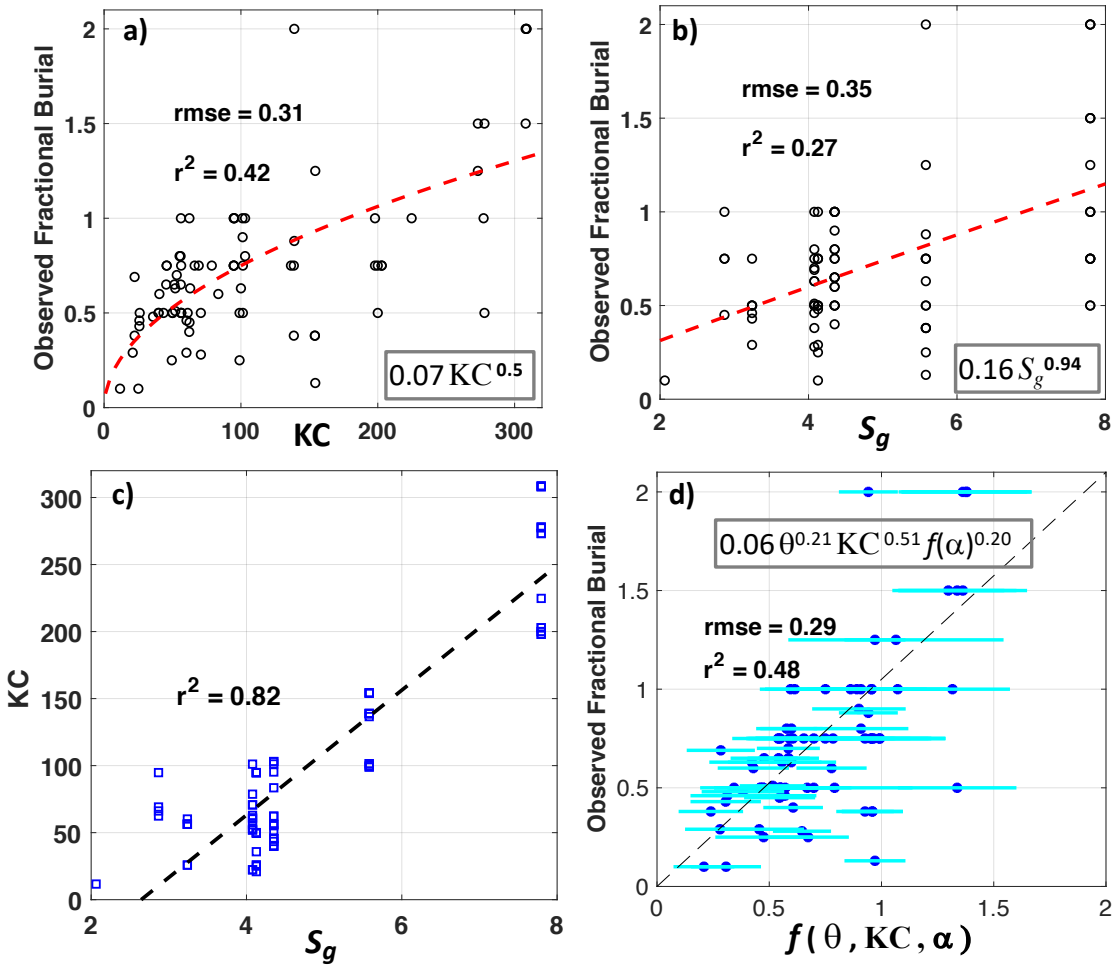

Figure 2.5. Parameterized relationships for LWE swash zone burial with *B* = 0 at start of run: a) power law fit of *B/D* at end of run to KC, b) power law fit of *B/D* to UXO normalized density, c) linear fit of UXO density to KC, d) multiple parameter power law relationship (95% C.I. marked as cyan bars)

However, note that a relationship with density alone captures a moderate amount of burial variability, as shown in Figure 2.5b (density represented by the UXO specific gravity $S_g = \frac{\rho_{obj}}{\rho_{water}}$), whereas parameterizations with UXO density examined by Friedrichs *et al.* [2016] revealed no significant relationship to burial under low to moderate wave forcing. Object density plays no role in the physics of scour burial; therefore, the dependence on density observed in the swash zone

indicates that processes such as bed fluidization are important. Unfortunately, analysis of the LWE data is complicated by the common correlation between UXO diameter and density: the smallest diameter UXO deployed (20 and 40 mm projectiles) are the most dense (Table 1.1). As diameter is the denominator in KC, density and KC become linearly related (plotted in Figure 2.5c) with r^2 = 0.82, making it difficult to separately discern the oscillatory flow effects from the influence of density in this data set for high-energy swash zone conditions.

A recomputed fit combining the θ and KC factors results in only a small improvement in the squared correlation coefficient over the fit to KC alone, resulting in r^2 = 0.47 (fit not shown) vs. r^2 = 0.42 noted above when fit only to KC. Several more complicated formulations for equilibrium burial were explored by Cristaudo & Puleo [2020], including factors for munition aspect ratio and the Iribarren number, which showed minimal improvement. In place of the aspect ratio, the factor representing the influence of angle of attack from Eq. (2.10) was used in the recomputed relationship,

$$B/D = a_6\theta^{b_6} KC^{c_6} f(\alpha)^{d_6} \qquad \text{Eq. (2.11)}$$

resulting in $\{a_6$=0.06, b_6=0.21, c_6= 0.51, and d_6= 0.2$\}$ plotted in Figure 2.5d, which also shows the 95% confidence intervals obtained with the swash data set. With an r^2 = 0.48, this 3-factor formula is the best combination found, yet still captures less than half of the observed variability for burial in the swash zone.

Because the LWE experiments were mostly conducted with limited run durations of 2.5 or 5 minutes, the recorded burial may not represent equilibrium conditions. However, there is no statistically discernable increase in burial for the longer runs. Time series data for burial was available in the swash zone from a 155 mm surrogate instrumented with photocells. These time series showed rapid burial, with B/D > 0.25 after no more than 30 s. Theoretical estimates for the time scale of scour have an inverse dependence on θ; between $\theta^{-1.5}$ and $\theta^{-2.02}$ [Demir and Garcia, 2007; Whitehouse, 1998]. With the very large θ in the swash zone, the time scale is expected to be shorter, therefore it is possible that the LWE run durations were actually long enough to reach equilibrium burial. Note that in the previous UnMES implementation to compute time-dependent burial, a time constant longer than theoretical is applied, based on evidence from surf zone field experiments [Traykovski and Austin, 2017] where a time scale on the order of tens of minutes was required to effect complete scour burial.

An implementation of the time-dependent scour algorithm used in the surf-zone version of UnMES, based on Eq. (2.9) but using the more rapid time scale, was applied to the LWE swash zone runs, and an estimated time-dependent burial, B_{t_pred}, was computed. The predicted scour burial was deeper than observed: 86% of predictions were fully buried, while only 22% runs were observed to exhibit complete burial. Given the large values of θ in the swash zone, it is not

surprising that burial is over-predicted by the surf-zone scour formulation. In a similar test, the extant migration distance algorithm in UnMES (described in Section 2.1.3) was applied, and strongly over-estimated *DistX* for LWE conditions. As expected, dominant processes in the swash zone, with intermittent strong uprush and backwash, are very different that those in the surf zone environment for both burial and mobility.

The UXO deployed in the deeper breaker zone were not reset in between runs, and depth of burial measurements could not be made as accurately underwater. Therefore, burial in the breaker zone was not analyzed.

2.3 Building and Testing an Expert System for the Swash Zone

In order to study UXO behavior during the Aberdeen LWE experiments, special instrumentation was installed [Bruder *et al.*, 2018], providing science-grade in-situ measurements of cross-shore flows in the swash zone. However, when using an expert system for coastal management problems, the real-world availability of environmental measurements must be considered. Analysis of swash zone munitions behavior in the previous sections made use of in-situ measurements, while, in a practical application, fluid velocity on the beach face will need to be estimated from operationally available observations, such as offshore wave conditions from NDBC buoys, or from video beach remote sensing techniques pioneered by Holman *et al*., [2015].

2.3.1 Modeling Swash Zone Conditions from Offshore Observations

Coastal engineers studying beach erosion have put substantial effort into understanding the empirical relationships between swash zone hydrodynamics and the offshore signficant wave height and length, H_0 and L_0, which are routinely monitored from NDBC buoys. These relationships usually also require knowledge of the foreshore bathymetry slope, as in the Iribarren number ξ.

A standard set of parameterizations to estimate the wave-forced time-averaged water level elevation (setup, η), the amplitude of time-varying fluctuations of swash (S), and their combined measure maximum runup (R) were determined by Stockdon *et al.* [2006] from an extensive set of field observations at several sites, largely obtained from video beach remote sensing [Holman *et al.*, 2015]. The complex hydrodynamic response in the swash zone was shown to require separation of wave energy into two spectral bands: at the incident (swell) wave frequency, S_{Inc}, and swash motions driven by infragravity waves, S_{IG}. These empirical relations have been applied in many large scale coastal impact studies, e.g. Vitousek *et al.* [2017], in spite of the modest correlation achieved by the Stockdon regressions (r^2 ranging from 0.44 to 0.65). Numerous recent studies have revisited this useful parameterization approach, proposing refinements and improvements that result in improved fit; however, a review by Gomes da Silva *et al.,* [2020]

points out that these more complex equations require additional measurements, such as details of the subaqueous bottom profile, or of the incident wave spectra; measurements that may not be readily available in coastal management practice. Many parameterized fits also do not perform robustly when applied to different sites. Puleo and Cristaudo [2020] concluded that even slight variations in local or offshore bathymetry, which alters wave shoaling and refraction, can influence the response of munitions on the beach face.

Several attempts to relate UXO burial to observed R from the LWE runs were attempted, but no significant correlation could be discerned. In spite of modest success in establishing engineering models to predict R from bathymetric slope and offshore waves, it is more difficult to determine the characteristic flow velocities in the swash zone. Application in UnMES, based on the relationships explored in Sections 2.1 and 2.2 requires an estimate of maximum swash velocity, which depends on the highly-asymmetric form of the uprush. Even the calculation of period-averaged velocity is problematic due to the transfer of energy from offshore wave peak frequency to infragravity motions that can dominate on many beaches. Fluid velocity does not appear to have been successfully extracted from video remote sensing time series. Instead, efforts to model flow velocity have been focused on using in-situ swash velocimeters to calibrate process-based numerical models that solve the nonlinear shallow water equations, an approach that would require substantially more investment for application at an UnMES site, including the development of bathymetry grids and boundary forcing.

These numerical models evolved from earlier work with the Rbeach model [Kobayashi *et al*. 1989, Raubenheimer 2002], to recent work with the phase-resolving SWASH model [Zijlema *et al.* 2011]. Alternatively, several possible versions, or modes, are available for Deltares XBeach, a model originally designed to simulate morphologic change at the timescale of storm events, but now extended to predict high frequency details when run in non-hydrostatic mode [Roelvink *et al.,* 2018]. For highly dissipative beaches, with small slopes ($\tan\beta \leq 1{:}50$), XBeach can be run in the more computationally efficient "surf-beat" mode to predict infragravity swash flows. A SERDP seed project is currently underway to test a suite of SWASH and XBeach implementations in order to understand the roles of wave asymmetry and offshore return flows that control UXO migration in the surf zone [Traykovski and Palmsten, 2020]. It is possible that such a study could be leveraged to run many cases of interest producing swash zone flows, and thereby build up the conditional probability tables needed for UnMES to relate offshore wave monitoring to flow in the swash zone. In the meantime, maximum swash velocity and dominant period at the beach face will be treated as input nodes for the swash zone implementation of UnMES.

2.3.2 Swash Zone Expert System: UnMES-SZ

The ability to accurately predict burial and migration in the swash zone, given our present state of knowledge, is constrained by the large observed variability reported in Sections 2.1 and 2.2, and

the inability to discriminate among several significant physical processes, given the limited data set, and complexity of the response. At this time, a No-GO decision to implement a swash zone version of UnMES would be appropriate. However, one advantage of the Bayesian Network approach is that poorly known or ambiguous processes can be modeled in a manner that quantifies the uncertainty. In this way, an expert system can be built, documenting the current level of understanding, and providing a framework to build upon when further research reveals new insights. Feedback from operational communities has affirmed that, rather than functioning with no information, decision makers value even uncertain guidance [e.g. NATO, 2007; Vitousek *et al.*, 2017]. While verifying the usefulness of this preliminary swash zone UnMES, progress can continue in several supporting areas that currently present a modeling challenge.

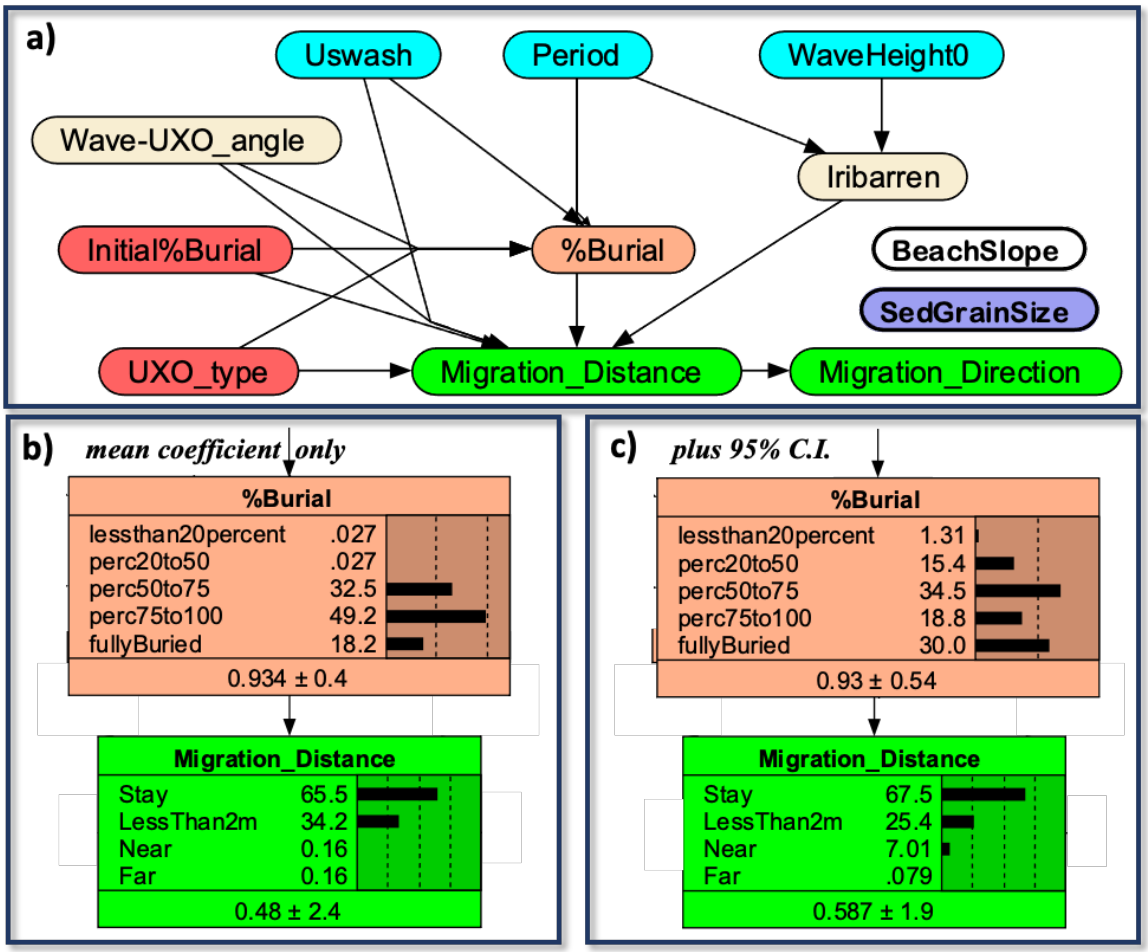

Figure 2.6. a) Diagram of Bayesian Network for UnMES-SZ.b) Example prediction of Percentage Burial and Migration Distance for 155 mm Howitzer, initially unburied under waves with H_0 ~1.5 m, T_p ~ 8 s, U*swash*, ~ 2 m/s for CPTs formed with best fit coefficients. c) Same as (b) except CPTs include 95% C.I. about best fit coefficients.

With this in mind, an exploratory BN for a swash zone version, UnMES-SZ, has been constructed, whose overall structure is diagramed in Figure 2.6a. The temporal construct, as for the Prototype

UnMES, represents the UXO response to a single storm event The required environmental inputs are U*swash*, the maximum uprush velocity representative of the storm event, T_p, the dominant period , and a median sand grain size and slope representative of the beach face. In addition, the offshore wave height is included to inform the estimate of ξ. The UXO type is described by the same node structure as used in the Prototype UnMES developed for the surf zone. The bin choices for both initial and predicted Percentage Burial are also the same as in the Prototype version. However, the migration distances are discretized at smaller intervals (bins), suitable for both the shorter distances within the swash zone, and the spatial scales of management concern in this area (shown in Figures 2.6b and c). In UnMES-SZ, "Stay" is defined as movement less than the UXO diameters. The state "Near" reports migration between 2 and 5 m, with the state "Far" assigned to any larger distance.

The physical relationships implied by the links between the nodes in UnMES-SZ are defined by the best empirical fits to the Aberdeen LWE observations obtained in the previous sections for migration and burial (Eqs. 2.5, 2.7, 2.11), augmented by gaussian stochastic spread representing the 95% confidence interval found for each coefficient in the equation, in an effort to include the present uncertainty for swash zone modeling. A comparison is presented in Figure 2.6 between the conditional probability tables resulting from using only the mean best fit coefficients (Figure 2.6b) and those computed with the additional uncertainty (Figure 2.6c). This example illustrates burial and migration predictions for a 155 mm howitzer type UXO ($\rho_{OBJ} = 4230$ kg/m^3) under moderate wave forcing. The overall results are similar: the mean % burial (93%) is that same, most UXO are predicted to be more than 3/4 buried, and most remained stationary. However, the spread is larger in Figure 2.6c; with the additional predictive uncertainty especially evident in the potential for less burial.

2.3.3 Application of UnMES-SZ

After implementing UnMES-SZ using the statistical relationships developed with the Aberdeen LWE data, probabilistic predictions can be compared to data from the 2018 field experiment at Wallops Island, where 115 cases of munition burial in the swash zone were recorded [Puleo and Cristaudo, 2020]. For the example comparison presented in Figure 2.7, only the burial observed for the larger munitions was used, since measuring accurate percentage burial for 20 mm and 40 mm projectiles is very difficult. The UXO_type input distribution shows the mix of munitions types deployed at Wallops Island. The initial burial input distribution reflects a combination of the deployed burial depths combined with the assumption that if migration was observed, then the burial became nil at some point in time. The predictions are driven by peak wave conditions observed during the field test in September and October: H_0 ~3 m, T_p between 10 to 15 s, U*swash*, ~ 2.5 m/s (not shown). UnMES-SZ predicts full burial for over half of the munitions, and over 80% will be more than 3/4 buried (Figure 2.7a), which is quite close to the observed results of 77% fully buried with 82% more than ¾ buried (Figure 2.7b).

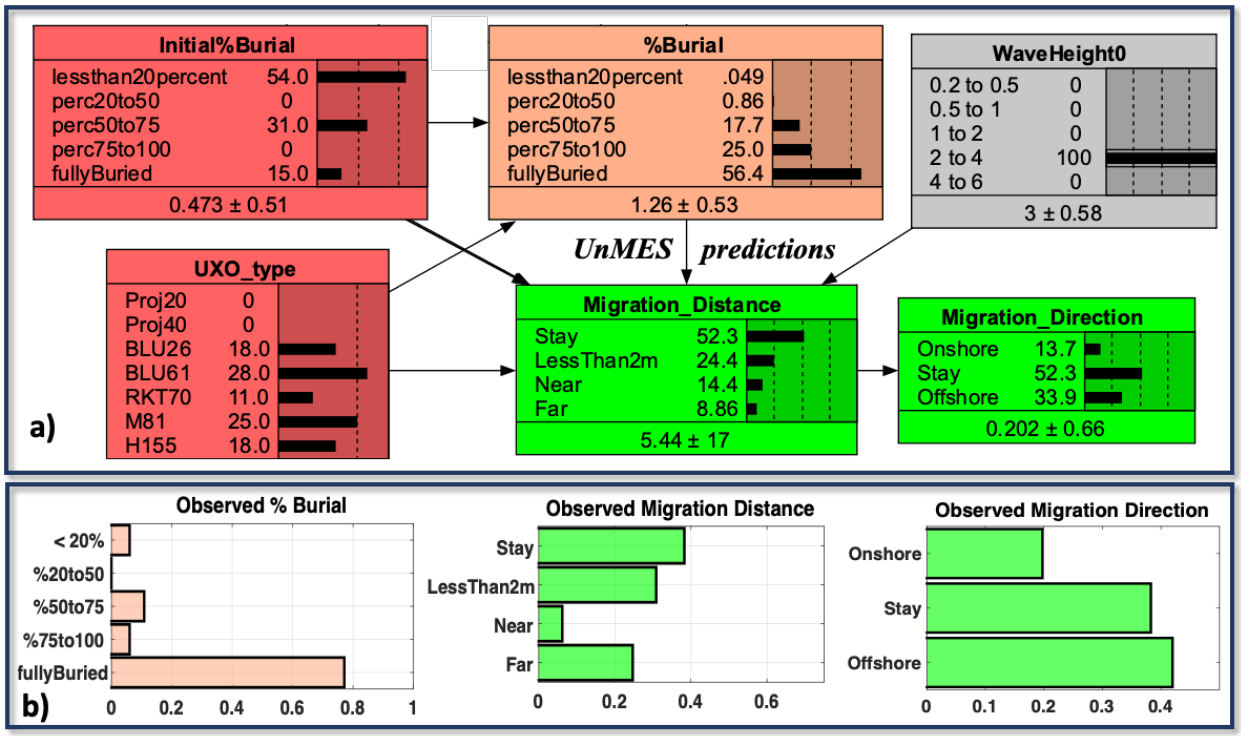

Figure 2.7 a) UnMES-SZ applied to conditions from Wallops Island 2018 field test. b) Histograms of observations from the Wallops Island field test [Puleo and Cristaudo, 2020].

For the migration results shown in Figure 2.7a, about half the munitions are predicted to remain in place, with another quarter moving less than 2 m. The Wallops Island data on migration also showed the preponderance of observations in the two smallest distance bins, but more "Far" displacements were measured than predicted. This is consistent with the conclusion in Section 2.1.3 that the empirical fit did an especially poor job at expressing large migration distances. Even with the additional spread provided by inclusion of the 95% C.I. about the coefficients, the variability is under predicted. Note that a few of the 81 mm mortar migration cases observed during the field test were for a surrogate with no fins, a UXO type not represented in the LWE training data. However, exclusion of these cases made little difference in the results, indicating that larger scale migration behavior may not be changed by the presence or absence of fins. For the UnMES-SZ prediction of Migration Direction, the probability distribution table (PDT) is based only on the summary statistics reported in Figure 2.1. In the field data histogram, onshore movement is seen to have been observed somewhat more frequently, representing one third of the mobile cases (approximately 20% of all cases).

Overall, UnMES-SZ trained with probabilities derived from the Aberdeen LWE statistics does a reasonable job of forecasting the generality of munitions behavior at the Wallops Island field site, albeit with some details not consistent. The forcing conditions at both Aberdeen and Wallops can be classified as moderate. It would be an important addition to the swash zone knowledge base to obtain observations in extreme storm conditions. During strong storms, changes in the

geomorphology of the beach face will likely be an important factor in burial. An Erosion/ Accretion node is not yet included in UnMES-SZ, but could eventually be populated by results from regional numerical models such as XBeach [Traykovski and Palmsten, 2020].

At this time UnMES-SZ, and UnMES in general, provide the best predictive modeling based on the data and models available and thus provide the state-of-the-art assessment of UXO burial and migration in the swash zone currently available for use by remediation site managers. Further improvements are contingent on the inclusion of results from additional studies, with several relevant funded SERDP projects currently underway.

3.0 Munitions in an Estuarine Environment

The geographically enclosed estuarine environment represents the opposite end of the wave energy spectrum from the swash zone, being sheltered from large ocean swell, and with limited fetch reducing local wind sea. The seabed composition in estuaries is largely made up of fine-grained silts and clays, in equilibrium with the low energy depositional environment [Dalrymple *et al*., 1992]. Constricted sections of the estuary can be subject to strong tidal currents where the fine grains are swept away, leaving a sandy area; but generally, the estuarine seabed will have a significant cohesive component. The characteristics of muddy seabeds are complex: the erodibility (potential for scour), and the sediment strength (resistance to penetration, i.e., the potential for impact burial) vary strongly with the local sand/mud fraction, and the history of consolidation [Thompson and Beasley, 2012].

Because of the prevalence of soft cohesive sediments, it is expected that impact penetration will be an important contributor to UXO burial in estuaries. Previous relevant research includes several studies sponsored by the Office of Naval Research (ONR) during the Mine Burial Program (MBP) with an experimental emphasis on the potential for munition burial upon initial impact with the seabed [Wilkins and Richardson, 2007; NATO, 2007]. In addition, the ONR MBP sponsored research on subsequent burial by scour [Trembanis *et al*., 2007], and included early work with the Bayesian Network approach [Rennie *et al*., 2007]. To understand burial and mobility of UXO in cohesive sediment, the SERDP project MR-2730 was undertaken, with multiple field experiments in Delaware Bay involving extended deployments of surrogate UXO [Trembanis and Duval, 2020]. Results from these studies will be used herein to construct a demonstration version of UnMES suitable for an estuarine environment, UnMES-ES. The next section discusses the preliminary Bayesian Network designed to represent the dominant environmental factors in estuaries. The following sections discuss the physics-based models developed to populate the conditional probability tables embodying burial behavior of UXO in that environment.
Note that no significant UXO mobility was observed during MR-2730, in concurrence with ONR MBP results showing that little migration occurs in the estuarine environment. Reasons for the lack of movement are discussed in the following sections.

3.1 Design of UnMES-ES

The preliminary Bayesian Network developed for UnMES-ES, illustrated in Figure 3.1, is derived initially from the Prototype surf zone version of UnMES [Rennie *et al*., 2019], excluding the nodes that represented geomorphologic behavior in non-cohesive sediments. Because variation in sediment composition is the dominant factor in estuaries, a new node is introduced representing sediment class. The underlying assumption that the UnMES BN represents a single location with a fixed water depth (h) remains. The types of sediment classes included represent the conditions at the two field experiment locations in the MR-2730 Delaware Bay project. During Fall 2017 and Spring 2018, deployments were at Site 1 in h = 4.5 m with muddy sand sediments. The following year the shallower (h = 3.5 m) Site 2 was studied, with softer sediments that were classed as sandy mud. A fine sand seabed class was sampled by geotechnical surveys near by the Delaware Bay study sites during SERDP MR20-1480 [Trembanis and DuVal, 2021]. To complete a representative range of estuarine sediments, a class representing very soft muds is included, as were studied in the York River during SERDP MR18-1233 [Stark *et al*., 2020]. In the spirit of the geotechnical sediment characterization approach being studied by MR20-1480, each class is assigned representation profiles of sediment strength and density, which are important parameters in modeling impact and subsequent burial (see Sections 3.2 and 3.3).

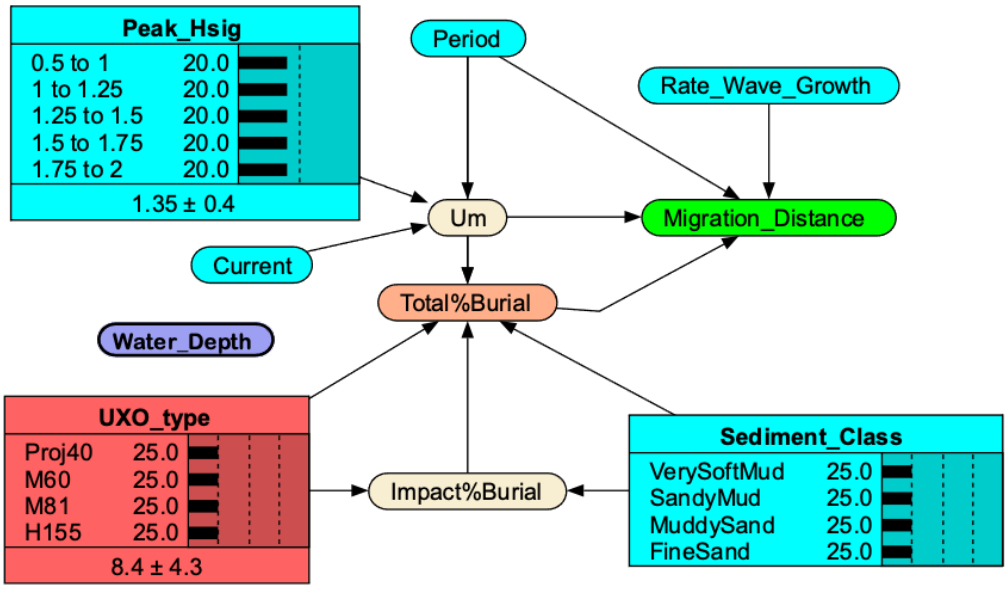

Figure 3.1 Bayesian Network for preliminary estuarine underwater munitions expert system, UnMES-ES.

The UXO types chosen for this demonstration UnMES-ES include the 81 mm mortar and 155 mm howitzer used in UnMES-SZ (Table 1.1), but both modified to be closer to the density of surrogate munitions deployed in MR-2730, (ρ_{obj} = 3700 and 3100 kg/m^3 respectively). In addition, a 60 mm mortar (ρ_{obj} = 3700 kg/m^3) was among the UXO studied during MR-2730. The 40 mm projectile

(ρ_{obj} = 5720 kg/m^3) used in UnMES-SZ was added to the UXO type node in order to include a higher density example. The value shown in the UXO_type node denotes the diameter (cm). The implementation code to build UnMES-ES maps each UXO type to its density. Additional information required about each UXO is an estimate of the mass offset from the geometric center, and whether or not the munition has fins, in order to determine the distribution of angle of attack during its water trajectory (Section 3.2).

The sheltered location and shallow depths of estuaries limit wave heights, so that the bins in the Peak_Hsig node can be reduced from those used in the surf zone UnMES. During MR-2730 field tests, the largest local H_s observed at the study site in the Delaware Bay during the storms of spring 2018 was < 1.9 m, while the offshore ocean waves peaked at H_0 = 4.4 m. Analysis of storm intensity and frequency confirm that a maximum bin of H_s = 2 m would cover most extreme storm waves within the Delaware Bay [Dohner, 2021]. Note that for this example UnMES-ES, the simplifying assumption is made that waves and current directions are generally orthogonal, and that the UXO orientation is unknown.

The Migration Distance node is retained in UnMES-ES, although no field data on UXO movement in estuaries has been observed. Minimal mobility is expected due to the likelihood of initial burial on impact, and subsequent moderate wave energy. The Prototype UnMES included a node predicting impact burial which was based on a simplified ballistic model [Rennie and Brandt, 2017] for high impact velocities, with the assumption that the seabed was medium dense sand. For softer estuarine sediments, very high impact velocity will almost always result in complete burial. For this implementation, impact modeling will focus on slow to moderate velocities.

3.2 Impact Burial in Estuarine Sediments

As discussed in Section 1, previous SERDP investigations of UXO burial focused on coastal regions where the seabed is largely sand, a non-cohesive granular medium that exhibits strong resistance to penetration. During ONR MBP field tests, it was shown that munitions falling through the water at terminal velocities (between 1 to 10 m/s) experienced minimal burial in sandy sediment. An early Navy model, IMPACT28 [Arnone and Bowen, 1980], was updated by Chu and Fan [2005] as IMPACT35, whose model results matched the observed penetration of less than 0.1*D* (i.e., < 10% burial) for a large surrogate munition dropped on medium sand. A review of the models available to predict impact burial in non-cohesive sediment was undertaken [Rennie and Brandt, 2017], with a focus on impact at very high impact velocity, such as could have occurred at former artillery and aerial bombardment ranges. Although high impact speeds may be relevant at some estuarine sites of interest, we will consider here the more common situation where munitions were released at modest initial speeds so that they impact the seabed at their terminal velocity in water.

3.2.1 Hydrodynamic Model for Impact Burial

The impact velocity of the UXO at the water-sediment interface is designated v_0. Field experiments sponsored by the ONR MBP showed that munitions falling at v_0 between 1 and 10 m/s could bury completely in very soft muds, or become partially buried in soft to medium cohesive sediments. Modest success was obtained in predicting observed burial penetration using the IMPACT28/35 models [NATO, 2007], whose code is largely devoted to calculating the orientation of the UXO (treated as a cylindrical shape) during its trajectory through the water and into the sediment. Substantial effort was made by ONR researchers to improve the models' ability to accurately reproduce details of the through-water trajectory in order to predict v_0 and the corresponding impact angle ϕ_0. However, the behavior of the munition's path through the water column can be extremely irregular and complex due to dynamic processes associated with unsteady flow separation, complicated by air entrainment when passing through the water surface [Chu *et al.,* 2010]. In a review of UXO burial modeling, Teichman *et al*. [2017] conclude that a hydrodynamics model's predictive ability will be limited by the unknown initial conditions at the waterline. For implementation in the estuarine version of the expert system, a very simple 1D hydrodynamic model is used to bound the possible ranges of impact velocity and angle, which are then treated probabilistically as detailed below.

For a given UXO type, v_0 is modeled assuming terminal velocity is reached at a balance between vertical velocity and hydrodynamic drag, approached exponentially from v_{00}, the velocity at the air- water interface [Teichman *et al*., 2017]. Here, UnMES-ES is simplified from the Prototype UnMES, replacing the Air Velocity node with the assumption that v_{00} is ~10 m/s. A simplified approach to estimating the terminal velocity in water starts with modeling two endpoints of the possible angle of attack: either nose down (ϕ_0 =0), or broadside (ϕ_0 = 90). For broadside, a hydrodynamic drag coefficient C_d = 0.8 is used; for a nose down cylinder C_d = 0.4, with a nose down streamlined tapered projectile having C_d = 0.13 [Green, 1984]. Based on the munition's L, *D*, and ρ_{obj}, an estimate is made of the UXO taper, and therefore the appropriate nose down drag coefficient to apply. Note that in the shallowest regions of the estuary, e.g., $h < 2$ m, the terminal velocity might not be reached, and the value of v_{00} continues to have some influence.

Given information about the center of mass (CoM) and presence of fins, a sensible probability distribution is designed to represent the angle of attack, and, therefore, the probability distribution of v_0. Figure 3.2 shows examples of the angle of attack and terminal velocity probability distributions for 4 example UXOs. The 155 mm howitzer (H155) is the heaviest, with the largest range for terminal velocity between broadside (v_0 ~ 2 m/s) and nose-down (v_0 ~ 10 m/s) shown in Figure 3.2b. In contrast, the smaller, less dense 60 mm mortar has a maximum velocity less than 6.5 m/s. Both mortars, the 60 mm (M60) and 81 mm (M81), have fins which promote a nose-

down attitude, although fin breakage is a possibility, resulting in the full range of possible angles [Chu *et al.*, 2011]. CoM values were available only for the mortar-style surrogates, with CoM offsets of approximately 12% and 10% of the UXO length for M60 and M81 respectively. These offsets are fairly large, in accordance with the observed behavior where the mortars, especially M60, were recorded as buried tilted nose-down. Given the CoM values, the angle probability shape (Figure 3.2a) assigned to M60 is slightly more nose-down than the 81 mm mortar. The 155 mm howitzer and 40 mm projectile are not finned, and are assigned small CoM offsets (~ 1%), so that a near-broadside attitude is more common.

Because of the large aspect ratio of the surrogate UXO used, the projected area of impact varies strongly with angle of attack and therefore significantly affects the sediment resistant force, as explained in the next section. The CoM value also influences the rotation of the UXO during the penetration into the sediment computed by the IMPACT28/35 models. At the moment, considering the lack of detailed knowledge of the water trajectory, no initial rotation rate is assigned at the water-sediment interface.

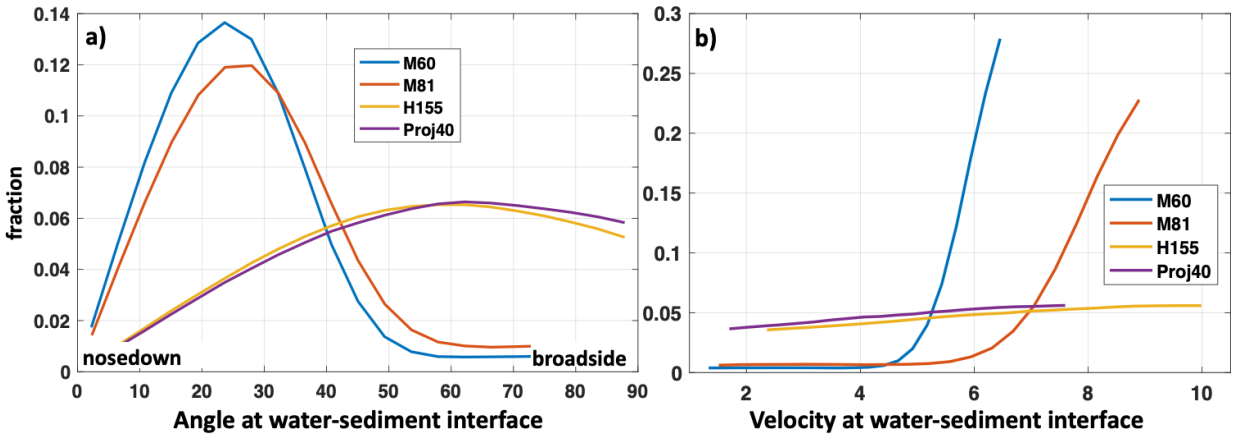

Figure 3.2 Probability distributions of angle of attack ϕ_0 and terminal velocity v_0 at impact with the seabed for four surrogate UXO types in UnMES-ES. Angle distribution is estimated from information about fins and center of mass.

3.2.2 Sediment Model for Impact Burial

While the speed and angle of the UXO at impact with the seabed are contributing factors in the degree of penetration, skillful prediction of impact burial depends overwhelmingly on accurate knowledge of sediment resistance to penetration. The key parameters controlling seabed penetration come from geotechnical and sedimentological characterization of the sediment. The most important of these parameters, undrained shear strength, s_u, describes the maximum stress that soil can sustain before rupture (shear failure) [Das, 1994]. Geotechnical measurements of s_u in marine sediments have traditionally been performed by laborious vane shear or cone

penetrometer tests [Thompson and Beasley, 2012]. Recent years have seen the development of dynamic penetrometers, which allow more rapid sampling of larger areas of the seabed. SERPD project MR18-1233 focused on rapid sediment strength measurement using a portable free fall penetrometer (PFFP) [Stark *et al*., 2020]. The procedure to estimate s_u from the deceleration record of a PFFP drop is essentially the inverse process to predicting depth penetration of an object given the shear strength. This is implemented in the IMPACT28/35 models as an iterative force balance through a sequence of thin sediment layers, where at layer *i*

$$F_i = W_i - Q_i - Fdrag_i - Fside_i \quad \text{Eq.(3.1)}$$

The penetrator buoyant weight, W_i, is resisted by a combination of $Fdrag_i$ and $Fside_i$, the friction along the side of the penetrator, as well as Q_i, the soil bearing resistance force. The resulting net downward force is F_i. If the load per unit area exceeds the bearing capacity, the upper layer fails and the object falls, at a slower velocity and reduced buoyant weight, to the next sediment layer to continue penetrating until the downward momentum is exhausted.

The translation between s_u and the bearing capacity is usually made using a simple empirical bearing (or cone) factor, N_k, which theoretically is expected to have some dependence on sediment characteristics and penetrator shape. The original value used in IMPACT28 was fixed at $N_k = 10$. Recent research with penetrometers reveals N_k varying from 7 to 13, with the value of $N_k = 12$ recommended as a conservative estimate [Stark *et al*., 2020]. Das [1994] noted that any uncertainty in bearing factor evaluation is likely overwhelmed by uncertainty in other environmental inputs.

The bearing factor applied to the shear strength predicts the load capacity of the sediment under static conditions, known as the quasi-static bearing capacity, QSBC:

$$QSBC = s_u N_k. \quad \text{Eq.(3.2)}$$

For the case of impact burial, the UXO can penetrate at a rapid initial rate, for example v_0=10 m/s. Since the sediment exhibits a nonlinear strain-rate dependent response, the dynamic bearing capacity, q_{dyn}, must be estimated by applying an appropriate strain rate factor (f_{SR}):

$$q_{dyn} = s_u N_k f_{SR}. \quad \text{Eq.(3.3)}$$

Multiplying q_{dyn} by the projected area A_p of the UXO impacting the sediment gives the soil bearing resistance force needed for Eq. (3.1):

$$Q = s_u N_k f_{SR} A_p \quad \text{Eq.(3.4)}$$

A major task of iterative sediment layer models like IMPACT28/35 is keeping track of the orientation of the UXO (treated as a cylindrical shape) as it falls and tilts, in order to compute A_p at each layer.

Investigation into the magnitude and form of the velocity dependent strain rate factor has been undertaken by many researchers, and is a particular focus of MR18-1233. The range of f_{SR} depends on the type of sediments being studied. A common equation for use in sediments with some sand fraction is the semi-logarithmic form suggested by Dayal and Allen [1973]:

$$f_{SR} = 1 + K \log_{10}(v_0/v_{q\text{-}s}), \qquad \text{Eq. (3.5)}$$

where $v_{q\text{-}s}$ is the reference penetration velocity representing quasi-static conditions ($v_{q\text{-}s}$ =0.02 m/s is the standard based on cone penetrometer testing). With a standard value for K = 1.25, f_{SR} = 4.4 at v_0 =10 m/s. Alternately, studies from soft sediments proposed to estimate the strain rate factor in power law form as

$$f_{SR} = (v_0/v_{q\text{-}s})^{\beta} \qquad \text{Eq. (3.6)}$$

where the exponent β ranges between $O(10^{-2})$ to $O(10^{-1})$. In the version of IMPACT28 used during ONR MBP, $1 < f_{SR} < 2$ for all values of s_u; while the IMPACT35 implementation used a slightly larger value with $1.5 < f_{SR} < 2.5$ [Rennie and Brandt, 2017].

Based on recent studies, it is clear that the applicable range of f_{SR} must be adjusted to the type of sediment under consideration. For extremely low shear strength, $s_u < 1$ kPa, Stark *et al*., [2020] conclude that no strain rate correction is required, i.e., β = 0, and f_{SR} = 1. However, in harder sediment with significant sand fraction, the shear resistance increases rapidly with v_0, exhibiting $f_{SR} > 6$ [Stark *et al*., 2012]. In order to train UnMES-ES, an impact burial model is implemented here using the sediment portion of IMPACT28 modified to apply varying ranges of f_{SR}, depending on the assigned sediment class. The applicable strain rate factors chosen for this preliminary version of UnMES-ES are illustrated in Figure 3.3, following Stark *et al*. [2012, 2020] and Kiptoo *et al.* [2019]. For this implementation using an updated version of IMPACT28, when applying Eq.(3.6) for the sediment class SandyMud, the value of β is treated stochastically, uniform over a range [0.01, 0.15], producing the band of values of f_{SR} shown in Figure 3.3 Understanding the effects of strain rate is an area of active research, and improved guidance for the estimation for f_{SR} is expected from upcoming SERDP projects.

Note that in previous applications of IMPACT28, it was observed that the model over predicted penetration into harder sediments [NAVO, 2007]. This over prediction would be corrected by the use of a varying form of the strain rate factor which increases with shear strength. In addition, to compute the training cases for UnMES-ES, IMPACT28 is implemented using the value for N_k as suggested by Stark *et al*., 2020].

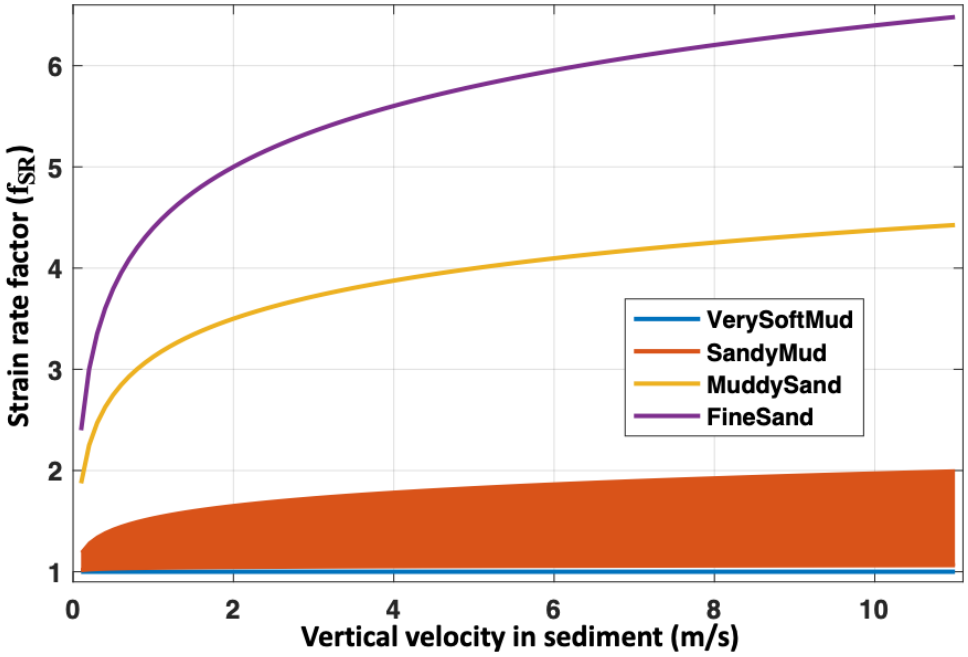

Figure 3.3 Strain rate factor variation with sediment class and vertical velocity proposed for use in UnMES-ES.

For each sediment class used in UnMES-ES, a representative profile of undrained shear strength s_u must be defined, s_u generally increasing with depth. The maximum s_u reached deeper in the profile is listed in Table 3.1. Estimated shear strength profiles for "Muddy Sand" and "Sandy Mud" are based on PFFP measurements made in the Delaware Bay at Site 1 and Site 2 respectively [Trembanis and Duval, 2020]. Shear strength was determined to be very low in the topmost ~ 5 cm of the seabed, then was observed to increase with depth. Stylized versions of this profile shape, shown in Figure 3.4, are used in the modified implementation of IMPACT28. A few PFFP drops sampled shear strength applicable to the sediment class "FineSand" in Delaware Bay, measuring very rapid increase to large $s_u > 20$ kPa, similar to s_u measurements made in sand during ONR MBP [Chu and Fan, 2005]. The profile for the sediment class "VerySoftMud" is derived from measurements in the York River reported in Stark *et al*. [2020], with maximum $s_u < 0.5$ kPa.

Table 3.1 Characteristics of Sediment Classes used in UnMES-ES

	Max Shear Strength	Max QSBC	Bulk Density	% Mud	Median grain size	τ_crit	Elastic Modulus E_{sed}
Sediment Class	**kPa**	**kpa**	**kg/m^3**		**mm**	**N/m^2**	**KPa**
Very Soft Mud	0.4	5	1500	99	0.005	0.11	0.1×10^4
Sandy Mud	0.9	11	1700	70	0.03	0.36	0.8×10^4
Muddy Sand	5.0	60	1900	30	0.09	0.72	1.2×10^4
Fine Sand	20.0	240	2000	1	0.2	0.16	3.0×10^4

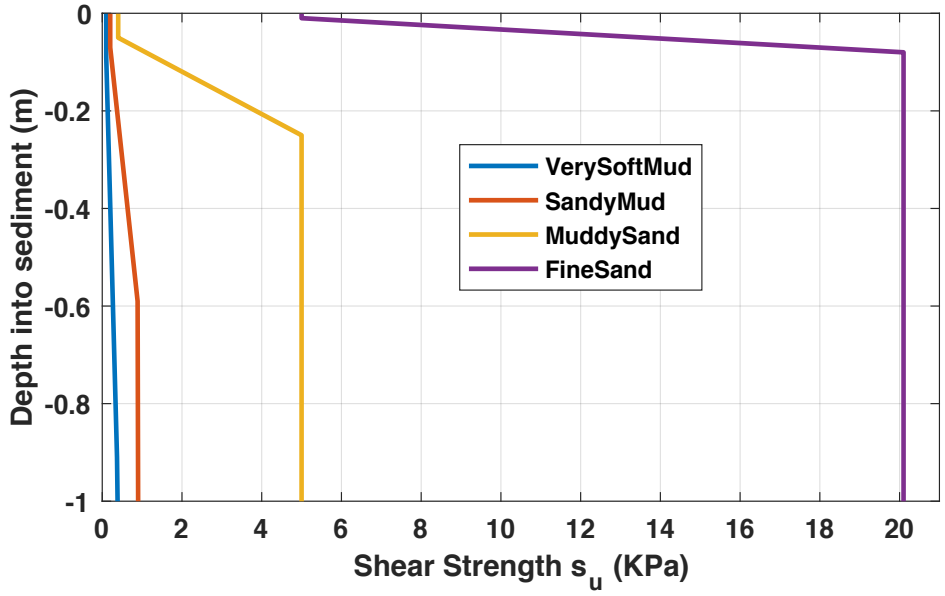

Figure 3.4 Stylized shear strength profiles representing the sediment classes in UnMES-ES.

3.2.3 Impact Burial Implementation in UnMES-ES

With probability distributions representative of the velocity and angle of impact for an example UXO type (Section 3.2.1), a version of the sediment portion of the model IMPACT28, modified as in Section 3.2.2, was run to estimate the degree of penetration for UXO into each sediment class. The fractional burial is calculated based on the percentage area of the UXO below the water-sediment interface. Figure 3.5 illustrates examples of impact attitude and the resulting burial for two example UXO types in the sediment class "Muddy Sand". The left panels (a & b) show burial for the M60 mortar which, with fins and a significant CoM offset, tends to fall nose-down, resulting in a smaller projected area A_p (Eq.3.4), and therefore increased burial. The right panels (c & d) show two draws from the H155 distributions, where a more broadside presentation results in less burial.

The modified IMPACT28 model is run in a Monte Carlo exploration of the water trajectory distribution and sediment resistance domains to produce training cases to build the Impact%Burial node in UnMES-ES. The overall distributions of impact burial following training of UnMES-ES for these two UXO types are shown in Figure 3.6. M60 UXO are predicted to be mostly or fully buried upon impact with Muddy Sand, whereas the H155 will often be only 1/2 to 3/4 buried (Figure 3.6b). The M81 burial distribution (not shown) lies in between the M60 and H155 results, while the 40 mm projectile has over 80% in the fully buried bin. Part of the large percentage burial predicted for the smaller munitions is due to the details of s_u profiles from the Delaware Bay, where a top layer of very soft mud overlays the stiffer sediment. The thickness of this soft layer is on the order of the diameter of the M60 and Proj40 UXO types, promoting complete burial when broadside.

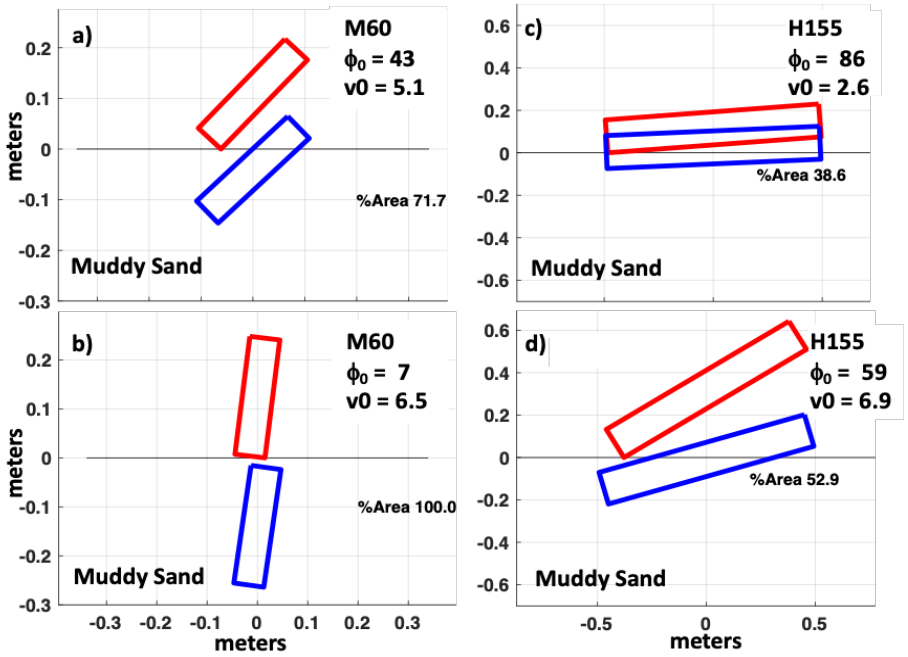

Figure 3.5 Modeled impact burial for M60 (a & b) and H155 (c & d) into sediment class Muddy Sand at two example angles of attack ϕ_0 (degrees) and terminal velocities v_0 (m/s).

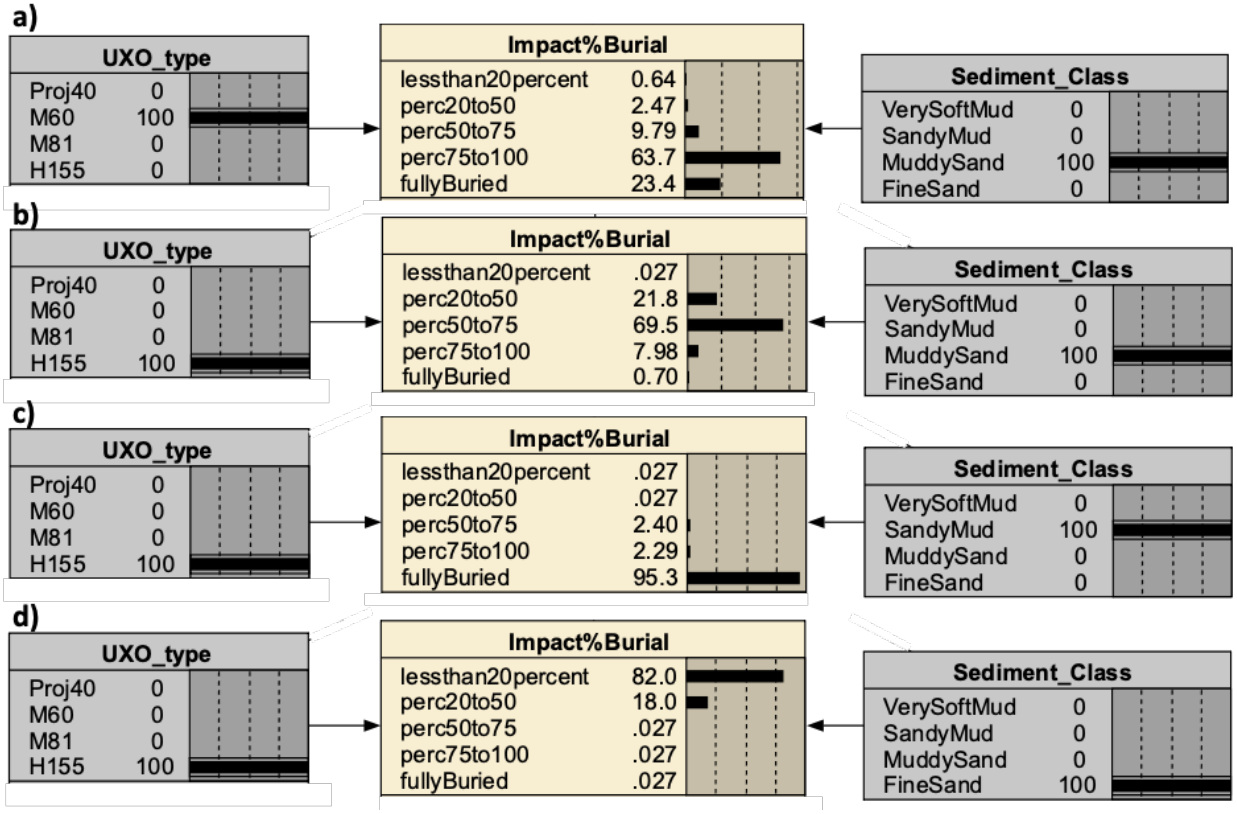

Figure 3.6 Probability Distribution Tables for impact burial in UnMES-ES: a) M60 and b) H155 in sediment class Muddy Sand; H155 in c) Sandy Mud and d) Fine Sand.

The sediment Muddy Sand is the only class for which there is a wide range of impact burial response. For softer sediments, almost all UXO are predicted to bury completely, for any given terminal velocity. The predictions for Sandy Mud are shown for the H155 UXO in Figure 3.6c: less than 6% of the distribution has any portion remaining unburied. In Very Soft Mud, over 99% of all UXO types fall in the fully buried bin (not shown). Representing the other extreme of shear strength in estuaries, predicted penetration in Fine Sand generally falls in the lowest bin at < 20% burial, shown in Figure 3.6d for H155. Proj40 burial in Fine Sand is very similar to the H155 probability distribution table (PDT), while the finned mortars are predicted to bury somewhat deeper, with the Impact%Burial PDT falling largely in the second bin (20 to 50% burial, not shown).

There are no observations of UXO impact burial from recent SERDP field tests to validate these predictions. However the modified IMPACT28 model results compare well with several scenarios documented during the ONR MBP program [NATO, 2007]. The surrogate UXO deployed in Delaware Bay during MR-2730 were placed by divers on the seabed to avoid initial burial. However, in realistic situations, munitions would have struck the seabed at the velocities modeled here. Given the prevalence of soft sediments in most estuaries, these results indicate that impact penetration will be the dominant burial process for UXO in an estuarine environment.

3.3 Scour Burial in Estuaries

The scour model published by Whitehouse [1998] provided the basis for ONR MBP modeling work [Trembanis *et al*., 2007], and was used by Trembanis and DuVal [2020] to estimate scour burial for conditions recorded during the MR-2730 field work. This engineering model was originally developed for piles and pipelines in non-cohesive sediment under steady flow conditions, and adjusted for use with free settling objects such as bottom-sitting munitions. An analysis of the sediment grain size at MR-2730 Site 1, represented by the sediment class Muddy Sand, had a mud fraction around 30%, while the Sandy Mud sediment at Site 2 consisted of closer to 70% mud. Trembanis and DuVal [2020] conclude that the scour process contributed to the burial observed at Site 1 during the periods of large storms, but did not appear to be a factor during calm periods at Site 1, or for any period at the more cohesive sediment at Site 2.

The main parameter in scour models is on the Shields number θ (Eq. 2.8), the ratio between destabilizing shear stress, and stabilizing weight of the sediment grains. The representative grain size d_{50} is listed in Table 3.1 for each sediment class modeled in UnMES-ES, while the grain density ρ_{sed} ranged from quartz (2650 kg/m^3) for sand to illite (2720 kg/m^3) for mud [Dohner, 2021]. The Whitehouse model formulation explicitly uses the critical shear stress, τ_crit, calculated for the sediment type, with shear stress τ equal to the numerator of θ in Eq. 2.8 scaled by ρ_w. Mud mixed in the sandy seabed significantly increases the τ_crit threshold for sediment mobilization. For a sediment consisting of 20% mud in sand, Whitehouse *et al.* [2000] found that the critical threshold was 5 times larger than for pure sand. The stress response is complicated, with the τ_crit threshold then decreasing for increased mud content over 20%. A theoretical curve of τ_crit based on percent mud fraction is presented in Dohner [2021]. Figure 3.7 plots the Whitehouse model fractional burial as a function of low to moderate shear stress for three example sediment classes implemented in UnMES-ES, with the applicable τ_crit listed in Table 3.1. There is a dramatic reduction in predicted scour burial with increased critical shear stress associated with intermediate mud fraction.

The scour burial model used in the Prototype surf zone version of UnMES was developed for non-cohesive sediment in combined waves and currents [Friedrichs *et al.,* 2016; Rennie *et al.,* 2017], as an empirical synthesis of scour observations of individual free settling objects, and is more appropriate to munitions in wave-dominated conditions. The Shields parameter factor was determined to be $B/D = 1.85\theta^{0.34} = f_\theta$ in Friedrichs *et al.* [2016]. The Friedrichs scour model computed for Fine Sand (plotted in Figure 3.7 as solid brown line) estimates somewhat less burial than the Whitehouse model. The Prototype version scour model also can include a dependence on the Keulegan-Carpenter number, (KC, Eq.2.8 & 3.7), which accounts for the effect of scour-

inducing vortices, whose size diminishes when the wave period gets smaller. The KC factor, proposed by the Friedrichs model to be applied as $B/D = f_\theta f_{KC}$, takes the form

$$f_{KC} = \min(0.103\,KC^{0.514}, 1.0) \qquad \text{with} \qquad KC = \frac{U T_P}{D}. \qquad \text{Eq. (3.7)}$$

For larger diameter UXO, D = 0.155, and short period waves, Tp = 5 s, $f_{KC} < 0.5$ for U < 0.7 m/s, meaning that scour burial is reduced by more than half in these conditions by the KC factor.

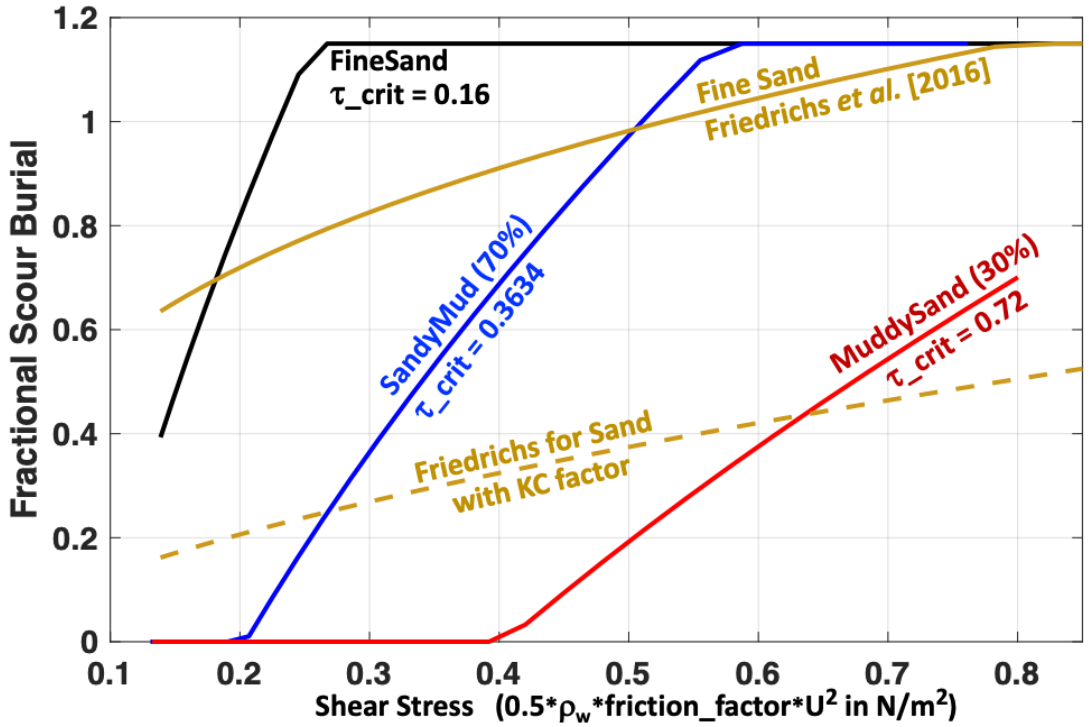

Figure 3.7 Scour burial computed by Whitehouse [1998] in FineSand (black), MuddySand (red), and SandyMud (blue) sediment classes. Friedrichs e*t al.* [2016] scour prediction without (solid brown) and with KC factor (dashed brown). Example is for H155 UXO over a range of shear stress corresponding to wave heights less than 0.5 m at MR-2730 Site 1 (*h* = 4.5 m).

Estuaries are generally sheltered from long-period swell, so that the peak wave period during storms is much shorter in estuaries than on the open coast. For the nor-easter storms recorded during the MR-2730 field tests in 2018, the peak period ranged from $3.5 < T_p < 6$ s, resulting in a KC factor that decreases the calculated wave-driven scour burial by a significant amount from the equilibrium scour burial computed for steady flow. The KC factor applied in the Friedrichs scour model for Fine Sand, overlaid on Figure 3.7 (brown dashed line), illustrates the reduction in predicted burial.

Therefore, the presence of cohesive sediment, along with the reduction in scour under short period waves, combines to produce strongly suppressed scour burial in estuaries. The implementation of scour modeling in UnMES-ES for Fine Sand will be based on the Friedrichs model, including the

KC factor. The other sediment classes with mud fractions will apply the Whitehouse model in order to specify the relevant τ_crit, and assume that the Friedrichs KC factor pertains. The wave nodes in UnMES-ES define the peak storm conditions to be modeled, noting that the initial burial percentage of the UXO is taken from the predicted Impact%Burial. Note that τ_crit for the sediment class Very Soft Mud shown in Table 3.1 is actually smaller than for sand [Whitehouse *et al*., 2000]. However, because impact in soft sediment generally leads to deep penetration, scour burial has little chance to play a role.

3.4 Burial by Settling and Fluidization in Cohesive Sediments

There are several other processes by which munitions can continue to bury into cohesive sediments over time. Trembanis and DuVal [2020] modeled the potential for munitions to slowly sink into the seabed, considering the static bearing capacity of the sediment, QSBC. The pressure exerted by the munition is calculated from the total weight from gravitation forcing minus buoyant forces. The effective pressure was modeled on the half surface of a rigid cylinder in contact with a deformable surface. To compute the contact surface of deformation, a high value for the elastic modulus of the UXO is assumed ($E_{obj} = 2.0x10^8$ KPa), while the sediment elastic modulus, E_{sed}, varies with the sediment class (see Table 3.1).

For implementation of burial by settling in UnMES-ES, the same approach is taken as in Trembanis and DuVal [2020], initially computing Hertzian cylindrical contact [Hertz, 1881], then with an iterative adjustment so that the pressure diminishes as the contact angle, ψ, widens with increased burial. The contact angle varies from Hertzian contact for UXO proud on the seabed, growing to 180º at half-burial, ψ increasing rapidly with even a small amount of burial (Figure 3.8a), resulting in a rapid decrease in pressure and, therefore, decreased settling depth. The depth of settling is determined as the point in the sediment profile where the contact pressure is balanced by the QSBC (Eq.3.2, Table 3.1 and Figure 3.4). The contact angle due to surface deformation alone, varying with E_{sed}, for a proud 155 mm cylinder is shown in Figure 3.8b. For extremely soft sediments, the munitions can become essentially half-buried by deformation alone, prior to settling *per se*. For stiffer sediment with significant sand content, initial ψ is smaller, with concomitant increase in pressure; however, these stiffer sediment generally have higher bearing capacity, so that the settling depth is limited.

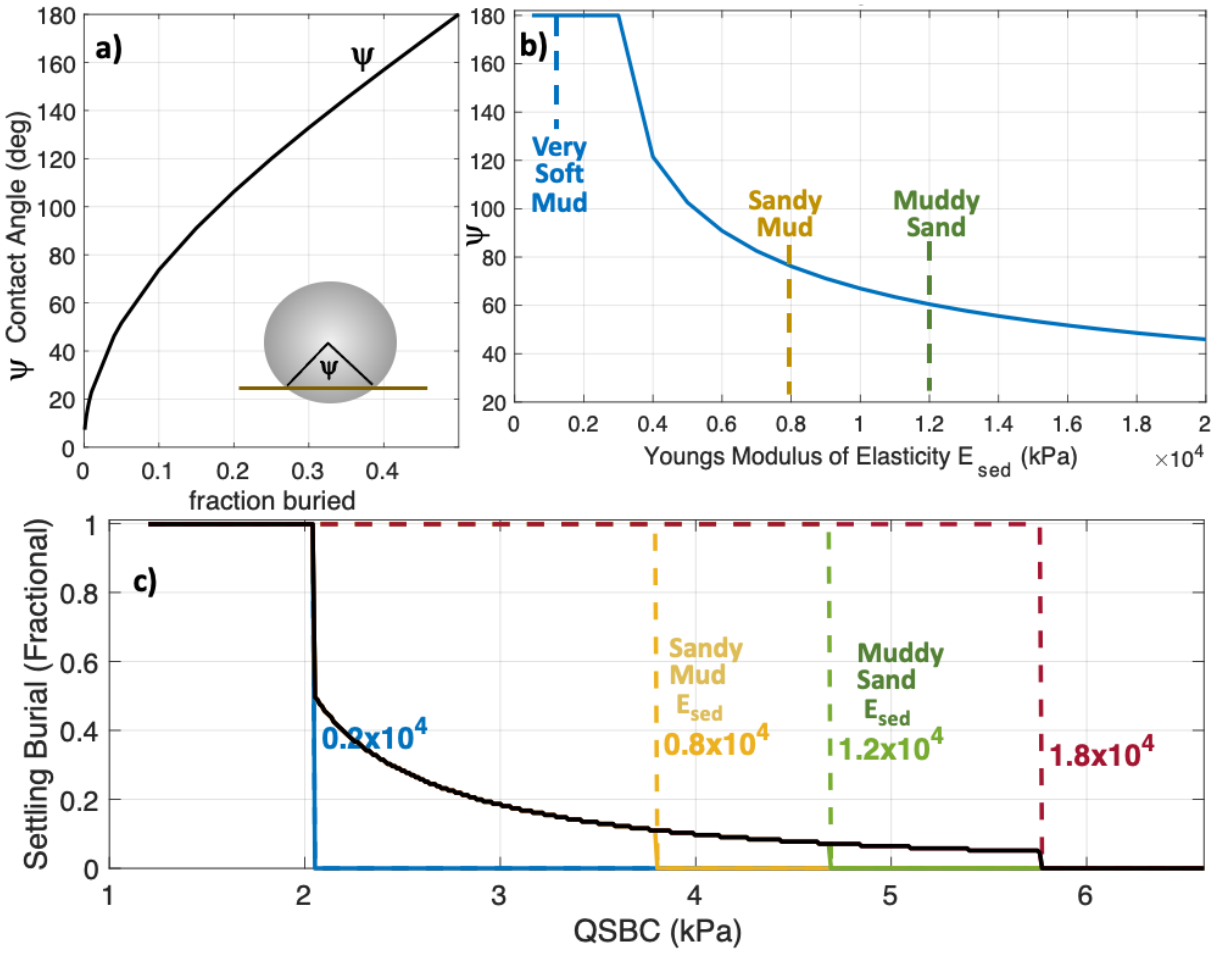

Figure 3.8 Sensitivity of settling burial model components: a) increase of contact angle with burial. b) Contact angle for initially proud cylinder depending on sediment elastic modulus, E_{sed}. c) Prediction of settling burial dependence for H155 on QSBC and E_{sed}, computed with (solid lines) and without (dashed lines) iterative adjustment of contact angle.

In Figure 3.8c burial from settling for H155, as computed with iteratively increasing ψ, is plotted (solid lines) versus bearing capacity for very soft to medium sediments. The profile of QSBC is assumed to be uniform over the depth of the munition, so that for extremely soft sediments (QSBC < 2 kPa), the munition will sink completely. For higher QSBC, settling will occur depending on E_{sed}. Without the iterative increase in ψ, the model would predict complete burial for all QSBC < 3.8 kPa for $E_{sed} = 0.8x10^4$ kPa, indicated by the yellow dashed line. In general, settling will be a negligible contribution for these small munitions in locations with sediment having surficial QSBC > 6 kPa, observing that bearing capacity generally increases with sediment profile depth. In an operational setting, the large majority of munitions will experience significant impact burial in softer sediments (Section 3.2); for most cases with Impact%Burial > 50. In these cases, initial ψ will be fixed at 180º, so that the contact pressure is minimized, and settling is suppressed. Note that results from the settling model in Trembanis and DuVal [2020] were based on measured PFFP

profiles of bearing capacity for which the surface-most (~ top 5 cm) values of QSBC are undefined, but were assumed to be vanishingly small, resulting in predictions of settling to ~ 5 cm even in sandy sediments.

A mechanism with the potential for further subsequent burial in estuaries may be fluidization of muds during storm events. Future investigations have been proposed to study this process, extending current models for fluid mud layer thickness under waves [e.g., Soltanpour *et al.,* 2009]. At present, no simple model for munitions burial under mud fluidization is available for inclusion in UnMES-ES. An analysis of the burial observations recorded during MR-2730 found a mix of results, depending on the sediment class and the level of storm activity [Trembanis and DuVal, 2020]. The deepest burial was reported at Site 2 (Sandy Mud class), where the surrogate UXO was buried between 20 to 30 cm beneath the seabed. Neither scour nor settling could account for such deep burial, leaving mud fluidization as the most likely mechanism.

No mobility of munitions was observed during the Delaware Bay field experiments, and no other relevant UXO motion data from estuarine environments are available to inform a modified migration model for use in UnMES-ES. Strong storm forcing was recorded during the MR-2370 field experiments without migration occurring; however, the potential for movement during more extreme conditions cannot be ruled out. Lacking additional information, the CPT for the migration distance node is constructed using the previous ad hoc mobility model as in the Prototype UnMES [Rennie *et al*., 2019]. Because the onset of mobility is extremely sensitive to burial degree (Section 2.1.1), migration is likely to be applicable only in locations with stiffer, sandy sediments where burial from both impact and settling is likely minimal.

4. Summary and the Way Forward

In accordance with availability of data sets and the state of model maturity for swash zone and estuarine processes, two different approaches have been undertaken to develop new versions of the underwater munitions expert system representative of these additional environments.

To comprehend patterns of burial and migration in the swash zone, empirical regressions with physically relevant parameters were fit to the LWE datasets obtained under SERPD MR-2503 [Puleo and Cristaudo, 2020; Cristaudo and Puleo, 2020]. These field experiments produced a set of observations large enough to provide a limited statistical description of UXO behavior under a range of moderate wave conditions. However, the overall regressions were weaker than the empirical fits used in the previous version of UnMES that characterized burial and migration in the shoaling/surf zone environment. To express this uncertainty, the Bayesian Network designated UnMES-SZ was populated with CPTs calculated from the regression with additional spread from Gaussian draws within the 95% confidence interval about each coefficient. The resulting predicted

PDTs have a broader shape than those for the shoaling/surf zone UnMES, representing the current lack of knowledge of burial and movement in this energetic environment.

Due to high variability in burial and migration response in the swash zone, it was not possible to discern definitive physical force balances. The complex forces driving UXO motion and burial on the beach face continue to be the subject of SERDP studies, with large-scale laboratory tests underway designed to differentiate the effects of munitions density and roughness; and to explore extreme forcing conditions that were not achievable at the LWE test site [Puleo, SERDP MR20-1094]. Results from these experiments will provide better insight into swash zone behavior of munitions during strong storms, which are of most concern to site managers as UXO burial and migration are significantly enhanced under storm conditions. Further laboratory and field observations of munitions on the beach face will clarify the aspects of the processes, and allow validation of useful models that reproduce a significant portion of the UXO behavior in the swash zone. However, the lack of reproducibility in UXO movement and burial as measured during the repeated LWE trials previously performed indicate that a stochastic approach may continue to be suitable.

An estuarine version of UnMES has been developed, that focused on the potential for UXO burial in varying sediment strengths, represented in UnMES-ES by four sediment classes whose characteristics are based on seabed measurements from SERDP project MR-2370 [Trembanis and DuVal, 2020]. Previous work in the coastal zone determined that scour was the dominant burial mechanism in sand, however the cohesive nature of estuarine sediments suppresses granular erosion. In estuarine muds, burial upon initial impact predominates. The numerical model for impact penetration used previously during the ONR MBP was simplified with a straightforward hydrodynamic model appropriate for a probabilistic approach [Teichman *et al.*, 2017], and updated to reflect recent research into the strain rate and cone factors applicable in an estuarine setting [MR18-1233, Stark *et al*., 2020]. A model for subsequent burial by settling was adapted from SERPD MR20-1480 [Trembanis and DuVal, 2021], with contact pressure adjusted as the munitions sink into the bed. Generally, it appears that settling will make only a small contribution to UXO burial; although it is difficult to distinguish settling from burial due to seabed fluidization after an extended length of time.

The predictions from all models for these estuarine burial mechanisms are strongly sensitive to the exact input of geotechnical sediment measurements, especially the depth variation of shear strength (bearing capacity). The ability to sample across the remediation site using freefall penetrometers (MR18-1233) is a convenient measurement technology necessary for useful burial predictions. Rapid site characterization using ship-mounted geophysical surveying is a viable goal, with initial steps undertaken by MR20-1480 to relate surficial geophysical properties to subsurface sediment geotechnical distributions, from which the sediment classes in UnMES-ES can be

estimated. In order to determine the burial potential for the smaller munitions of concern, measurement of geotechnical properties in the uppermost seabed layer needs to be improved. This is a specific goal for the PFFP development under MR18-1233.

To be accepted for operational use by the user community, the Underwater Munitions Expert System needs a verified track record of successful application and repeated validation of UXO burial and migration predictions under relevant environmental conditions. Much progress has been made, so that UnMES-SZ and UnMES-ES, as presented here, are expert systems that provide a synthesis of current knowledge about UXO behavior in the swash zone, and in estuaries. However, overall, the level of validation currently achieved for UnMES is not fully satisfactory, especially in these complex environments. Compared to the accuracy and detail of prediction shown for the Prototype surf zone version of UnMES [Rennie *et al*., 2019], the swash and estuarine expert systems are not suitable for trial operational application at this time (a No-GO decision for release of UnMES-SZ and UnMES-ES). However, these BN demonstrate some useful predictive skill, and provide the basis on which to build improved networks. It is hoped that this report will give guidance to where future research and validation efforts would best be focused.

In summary, the essential area of research needed to be able to effectively model the swash zone are observations of UXO behavior under strong storm waves, concurrent with measurements of the near field beach face geomorphic changes. This is best obtained in a large-scale laboratory setting. Analyses of data from recently developed "smart" surrogate munitions will provide details of the response, in order to understand the relative contribution of different forces and their timing. Of particular importance is the ability to predict whether onshore or offshore motion will predominate. Due to the complex conditions in the swash zone, repetition of sufficient number of measurements are required to capture the statistics sufficient to build a useful probabilistic model of UXO burial and migration. At present, the simple fits incorporated in UnMES-SZ account for less than half of the observed variability in the swash zone, as compared to the Prototype surf zone UnMES which comprehended more than 3/4 of the measured variation. Also, UnMES-SZ does not yet include the breaker zone data which was less comprehensive than the swash zone measurements. Under strong waves, UXO burial and migration in the breaker zone will likely increase, and needs to be understood for a comprehensive expert system covering the surf zone to the beach face. The recent project undertaken by Traykovski [SERDP MR21-1341] focusing on shoaling wave forcing in very shallow water could provide the link between the regions.

Estuarine field data provided by Trembanis and Duval [2020] encompassed fairly strong wave conditions, although UXO behavior remains to be studied in estuarine regions where significant currents can combine with waves under certain storm conditions. There may be some useful overlap with the riverine studies begun by Duval [SERDP MR21-117]. The potential for scour or settling burial in cohesive sediments, at present addressed by a combination of theory and

extrapolation of simple engineering models, may be directly studied in a laboratory setting, as could the more concerning problem of burial by mud fluidization. The predominance of impact burial in soft sediments has not yet been addressed by the SERDP field work, however, the current focus on geotechnical characterization provides the necessary environmental input. The next step to improve estuarine impact burial modeling would be a validation field test designed to promote acceptance of UnMES-ES predictions by the user community.

Literature Cited

Arnone, RA, LE Bowen, 1980. Prediction of the Time History Penetration of a Cylinder Through the Air–Water–Sediment Phases, Naval Coastal Systems Center, Panama City, FL, Report T34.

Bruder, B, D Cristaudo, JA Puleo, 2018. Smart surrogate munitions for nearshore unexploded ordnance mobility/burial studies, *IEEE J. of Oceanic Eng.,* 99, 1-20.

Calantoni, J, 2018. "Long Time Series Measurements of Munitions Mobility in the Wave-Current Boundary Layer," SERDP In-Progress Review, May 2018.

Cataño-Lopera, YA, García, MH, 2007. Geometry of scour hole around, and the influence of the angle of attack on the burial of finite cylinders under combined flows, *Ocean Engineering* 34(5). 856-869.

Chu, PC, C Fan, 2005. "Prediction of Falling Cylinder Through Air-Water-Sediment Columns," *J. Appl. Mech*., 73, 300-314.

Chu, P, C Fan, PR Gefken, 2010. "Diagnostic---Photographic Determination of Drag/Lift/ Torque Coefficients of a High Speed Rigid Body in a Water Column," *J. Appl. Mech*., 77, 011015-1-15.

Chu, PC, J M Bushnell, C Fan, WP Watson, 2011. "Modeling of Underwater Bomb Trajectory for Mine Clearance," *J. Defense Modeling and Simulation, 8*(1), 25-36.

Cristaudo, D, Puleo JA, 2020. "Observation of munitions migration and burial in the swash and breaker zones," Ocean Engineering, Vol 205, 107322, 2020.

Dalrymple, SW, BA Zaitlin, and R Boyd, 1992. Estuarine facies model: Conceptual basis and stratigraphic implications, *J. Sediment. Petrol.*, **62**(6), 1130–1146.

Das, BM, 1994. Principles of geotechnical engineering, 3rd edition, PWS-Kent Publishing Company, Boston.

Dayal, U, and Allen, JH, 1973. Instrumented impact cone penetrometer. Canadian Geotechnical Journal, 10(3), 397-409.

Demir, ST, García, MH, 2007. Experimental Studies on Burial of Finite-Length Cylinders under Oscillatory Flow. *Journal of Waterway, Port, Coastal, and Ocean Engineering* 133, 117–124.

Dohner, S, 2021. Estuarine Morphodynamic Response and Recovery to Extreme Events *(In Press)*. Dissertation for Ph.D. Submitted to the University of Delaware.

Gomes da Silva, P, G Coco, R Garnier, AHF Klein, 2020, "On the prediction of runup, setup and swash on beaches", *Earth-Science Re*views, 204, 103148.

Green, AW, 1984. "Bulk Dynamics of the expendable bathythermograph (XBT), *Deep Sea Research*," *31*, 415-426.

Fawcett, T, 2006. Introduction to ROC Analysis, *Pattern Recognition Letters*, 27 (8), 861-874.

Friedrichs, CT, Rennie, SE, Brandt, A, 2016, Self-burial of objects on sandy beds by scour: A synthesis of observations, *Scour and Erosion*. CRC Press, 179–189.

Hertz, H, 1881. On the contact of elastic solids. In *Miscellaneous Papers* (MacMillan, New York, 1881/1896).

Holman, RA, Haller, MC, Lippmann, TC, Holland, KT, Jaffe, BE, 2015. Advances in nearshore processes research: four decades of progress, Volume 83, Issue 1, *Shore & Beach*, pp 39-52.

Kiptoo, D, Stark, N, Massey, G, Wright, C, and Friedrichs, C, 2019. Rapid geotechnical characterization of seafloor sediments at the Potomac River, Maryland, using a novel assessment framework based on portable free fall penetrometer measurements. SERDP/ESTCP Symposium 2019, December 3-5, 2019, Washington, DC.

Kobayashi, N, DeSilva, GS, and Watson, KD, 1989. "Wave transformation and swash oscillation on gentle and steep slopes." J. Geophys. Res., 94(C1), 951–966.

NATO Naval Armaments Group, Maritime Capability Group 3, Mine Countermeasures and Harbour Protection, 2007. Final Report by Specialist Team for Sea Mine Burial Expert System (SMBES), NATO Document AC/141(MCG/3)D(2007)0001, NATO Unclassified.

Nielsen, P, 1993. Coastal Bottom Boundary Layers and Sediment Transport, *Advanced Series on Coastal Engineering*. World Scientific Publishing Company.

Puleo, JA, Holland, KT, 2001. Estimating swash zone friction coefficients on a sandy beach. *Coastal Engineering* 43, 25–40.

Puleo, JA, Cristaudo, D, 2020. Quantification of Hydrodynamic Forcing and Burial, Exposure and Mobility of Munitions on the Beach Face, Final Report for SERDP Project MR-2503.

Puleo, JA, Cristaudo, D, Torres-Freyermuth, A, Masselink, G, Shi, F 2020. "The role of alongshore flows on inner surf and swash zone hydrodynamics on a dissipative beach," *Continental Shelf Research*, 201, 104134.

Raubenheimer, B, 2002. Observations and predictions of fluid velocities in the surf and swash zones. Journal of Geophysical Research 107 (C11), 3190, http://dx.doi.org/ 10.1029/2001JC001264.

Rennie SE, A Brandt, N Plant, 2007. A Probabilistic Expert System Approach for Sea Mine Burial Prediction, *IEEE Journal of Oceanic Engineering*, Vol. 32, No.1, *Special Issue on Mine Burial*, 260–272, Jan. 2007.

Rennie SE, A Brandt, 2017. "Status of Underwater Impact Penetration Modeling for use in the Underwater Munitions Expert System," Johns Hopkins University/Applied Physics Laboratory, FPS-T-17-0456, SERDP Interim Report for MR-2645, November 2017.

Rennie, SE, Brandt, A., Friedrichs, CT, 2017. "Initiation of motion and scour burial of objects underwater", *Ocean Engineering, 131*, 282–294. dx.doi.org/10.1016/j.oceaneng.2016.12.029.

Rennie SE, A Brandt, JG Ligo, 2019. "Prototype Underwater Munitions Expert System: Demonstration and User's Guide," Johns Hopkins University/Applied Physics Laboratory, FPS-R-19-0695, SERDP Guidance Document, MR-2645, November 2019.

Roelvink, D, McCall, R, Mehvar, S, Nederhoff, K, Dastgheib, A, 2017. Improving predictions of swash dynamics in XBeach: the role of groupiness and incident-band runup. *Coastal Engineering*, 1–21.

Soltanpour, M, Haghshenas, SA, and AJ Mehta, 2009. Fluidized Mud-Wave Interaction under Regular and Irregular Waves. *Journal of Coastal Research* 25 (3), pp. 616-626.

Soulsby, R, 1997. Dynamics of Marine Sands, London: Thomas Telford.

Stark, N, Wilkens, R, Ernstsen, VB, Lambers-Huesmann, M, Stegmann, S, & Kopf, A, 2012. Geotechnical properties of sandy seafloors and the consequences for dynamic penetrometer interpretations: quartz sand versus carbonate sand. Geotechnical and Geological Engineering, 30(1), 1-14.

Stark, N, GM Massey, CT Friedrichs, 2020. "Improved Penetrometer Performance in Stratified Sediment for Cost-Effective Characterization, Monitoring and Management of Submerged Munitions Sites," SERDP Project MR18-1233 Final Report.

Stockdon, HF, Holman, RA, Howd, PA, Sallenger, AH, 2006. Empirical parameterization of setup, swash, and runup. Coast. Eng. 53, 573–588. https://doi.org/ 10.1016/j.coastaleng.2005.12.005.

Sumer, BM, Fredsoe, J, 1990. "Scour Below Pipelines In Waves", *Journal of Waterway, Port, Coastal, and Ocean Engineering*, Vol. 116, No. 3, 307-323.

Teichman, JA, J Macheret, SM Cazares, 2017. UXO Burial Prediction Fidelity, Institute for Defense Analyses, IDA NS D-8616.

Thompson, D and Beasley, DJ, 2012. *Handbook for Marine Geotechnical Engineering*, NAVFAC SP-2209-OCN, Naval Facilities Engineering Service Center, Port Hueneme, CA, February 2012.

Traykovski, P, T Austin, 2017. Continuous Monitoring of Mobility, Burial and Re-exposure of Underwater Munitions in Energetic Near-Shore Environments, SERDP Project MR-2319 Final Report.

Traykovski, P, Jaffre, F, 2020. Rapid Response Surveys of Mobility, Burial and Re-exposure of Underwater Munitions in Energetic Surf-Zone Environments and Object Monitoring Technology Development, SERDP Project MR-2729 Final Report.

Traykovski, P, Palmsten, M, 2020. Wave Resolved and Averaged Numerical Modelling of UXO Migration, SERDP Proposal MR21-S1-1341.

Trembanis, AC, CT Friedrichs, MD Richardson, P Traykovski, PA Howd, PA Elmore, and TF Wever, 2007. Predicting seabed burial of cylinders by wave-induced scour: Application to the sandy inner shelf off Florida and Massachusetts, *IEEE Journal of Oceanic Engineering*, Vol. 32, No.1, *Special Issue on Mine Burial*, 167–183, Jan. 2007.

Trembanis, A, DuVal, C, 2020. Unexploded Ordnance Characterization and Detection in Muddy Estuarine Environments, SERDP MR-2730 Final Report.

Trembanis, A, DuVal, C, 2021. Further Examining the Role of Cohesive Sediments in Munitions Mobility through Additional Infield Deployment of Smart Munitions and Application of a SERDP-developed Penetrometer, SERDP MR20-1480 Final Report.

Vitousek, S, Barnard, P, Fletcher, C, N Frazer, L Erikson, CD Storlazzi, 2017. Doubling of coastal flooding frequency within decades due to sea-level rise. *Sci Rep* **7,** 1399.

Whitehouse, R, 1998. Scour at marine structures. London: Thomas Telford.

Whitehouse, R, Soulsby, R, Roberts, W, Mitchener, H, 2000. Dynamics of Estuarine Muds. A Manual for Practical Applications. HR Wallingford Report SR527, Wallingford, Oxon.

Wilkins, RH, and M Richardson, 2007. "Mine Burial Prediction: A Short History and Introduction", IEEE Journal of Oceanic Engineering, Vol 32, No. 1, *Special Issue on Mine Burial*.

Zijlema, M, Stelling, G, Smit, P, 2011. SWASH: an operational public domain code for simulating wave fields and rapidly varied flows in coastal waters. *Coastal Engineering* 58, 992–1012.